Environ Earth Sci (2013) 70:3797–3816
DOI 10.1007/s12665-013-2724-1

THEMATIC ISSUE

Unconventional reservoir potential of the upper Permian Zechstein Group: a slope to basin sequence stratigraphic and sedimentological evaluation of carbonates and organic-rich mudrocks, Northern Germany

Ursula Hammes · Michael Krause · Maria Mutti

Received: 16 November 2012 / Accepted: 6 August 2013 / Published online: 27 September 2013

Abstract The Late Permian Zechstein Group in northeastern Germany is characterized by shelf and slope carbonates that rimmed a basin extending from eastern England through the Netherlands and Germany to Poland. Conventional reservoirs are found in grainstones rimming islands created by pre-existing paleohighs and platform-rimming shoals that compose steep margins in the north and ramp deposits in the southern part. The slope and basin deposits are characterized by debris flows and organic-rich mudstones. Lagoonal and basinal evaporites formed the seal for these carbonate and underlying sandstone reservoirs. The objective of this investigation is to evaluate potential unconventional reservoirs in organic-rich, fine-grained and/or tight mudrocks in slope and basin as well as platform carbonates occurring in this stratigraphic interval. Therefore, a comprehensive study was conducted that included sedimentology, sequence stratigraphy, petrography, and geochemistry. Sequence stratigraphic correlations from shelf to basin are crucial in establishing a framework that allows correlation of potential productive facies in fine-grained, organic-rich basinal siliceous and calcareous mudstones or interfingering tight carbonates and siltstones, ranging from the lagoon, to slope to basin, which might be candidates for forming an unconventional reservoir. Most organic-rich shales worldwide are associated with eustatic transgressions. The basal Zechstein cycles, Z1 and Z2, contain organic-rich siliceous and calcareous mudstones and carbonates that form major transgressive deposits in the basin. Maturities range from over–mature (gas) in the basin to oil-generation on the slope with variable TOC contents. This sequence stratigraphic and sedimentologic evaluation of the transgressive facies in the Z1 and Z2 assesses the potential for shale-gas/oil and hybrid unconventional plays. Potential unconventional reservoirs might be explored in laminated organic-rich mudstones within the oil window along the northern and southern slopes of the basin. Although the Zechstein Z1 and Z2 cycles might have limited shale-gas potential because of low thickness and deep burial depth to be economic at this point, unconventional reservoir opportunities that include hybrid and shale-oil potential are possible in the study area.

Keywords Upper Permian Zechstein Group Northern Germany · Unconventional reservoir potential · Mudrock analyses · Sequence stratigraphy · Carbonate and mudrock facies

U. Hammes (✉) · M. Krause · M. Mutti
Institute for Earth and Environmental Sciences, University of Potsdam, Karl-Liebknecht-Str.24-25, 14476 Potsdam, Germany
e-mail: hammesu@gmail.com

U. Hammes
Bureau of Economic Geology, The University of Texas, 10100 Burnet Rd, Austin, TX 78746, USA

Introduction

A sedimentologic and sequence stratigraphic evaluation of the Upper Permian Zechstein Group in the northern German states of Brandenburg and Mecklenburg-Vorpommern was conducted to evaluate the unconventional reservoir potential of slope and basinal deposits for mudrocks and carbonates of the lower portion of the Zechstein units (Z1 and Z2 cycles; Richter-Bernburg 1955, 1982). The lower unit of the Zechstein Group, namely the Stassfurt Carbonates (Ca2) has been a prolific conventional exploration target in the North German Basin of the German States of Schleswig–Holstein, Niedersachsen, and in the Netherlands, England, and Poland. Recent interest through the

unconventional shale-gas and shale-oil boom in the USA (e.g., Barnett, Haynesville, Eagle Ford, Marcellus, Utica, and Bakken Shales) encouraged many oil companies to investigate the shale-gas and shale-oil potential in Europe. Previous evaluation of the shale-gas potential of the Zechstein Z2 Stassfurt basinal mudstones in the State of Brandenburg by Hartwig and Schulz (2010) precluded the occurrence of commercial shale-gas reservoirs in the basinal Ca2 mudstones because of low TOC, thickness limitations, and gas-prone kerogen type II/III. However, a comprehensive study of the unconventional reservoir potential and sequence stratigraphy and facies of the Z1 and Z2 in the Brandenburg and Mecklenburg-Vorpommern area is lacking to date. In this study, additional data was collected to evaluate the unconventional reservoir potential of the northern and southern slope and other parts of the basin including Z1 and Z2 Zechstein cycles (Richter-Bernburg 1955, 1982). Source-rock potential of the mudrocks of the Kupferschiefer (e.g., Bechtel et al. 2000) and laminated mudstones of the Ca2 (e.g., Karnin et al. 1996; Müller et al. 1993) exists and might be accessed for unconventional reservoir potential. Therefore, a comprehensive data set, consisting of cores and logs, was gathered from the geological surveys of Brandenburg and Mecklenburg-Vorpommern with the goal to generate transects across different stratigraphic intervals and depositional settings spanning geographically from the northern to the southern rims of the northern German Southern Permian Zechstein basin (Fig. 1). The specific objectives are to document sedimentary features of the mudrocks and the carbonates, to identify stratigraphic sequences, to conduct geochemical analyses, and to evaluate the unconventional reservoir potential of the slope and basinal mudstones.

Geologic setting

The study area lies within the Southern Permian Basin that extended from Poland through Germany, Netherlands into England in an east–west direction (Fig. 1; e.g., Ziegler 1990; Wagner and Peryt 1997; Lokhorst 1997; Geluk 2007). The North German Basin, which is part of the Central European Basin System, developed as a foredeep during Early Paleozoic Variscan orogeny as a result of regional thermal destabilization and transtensional stress-field. Wrench-related movement along NNE–NNW oriented fault systems in the late Carboniferous followed by

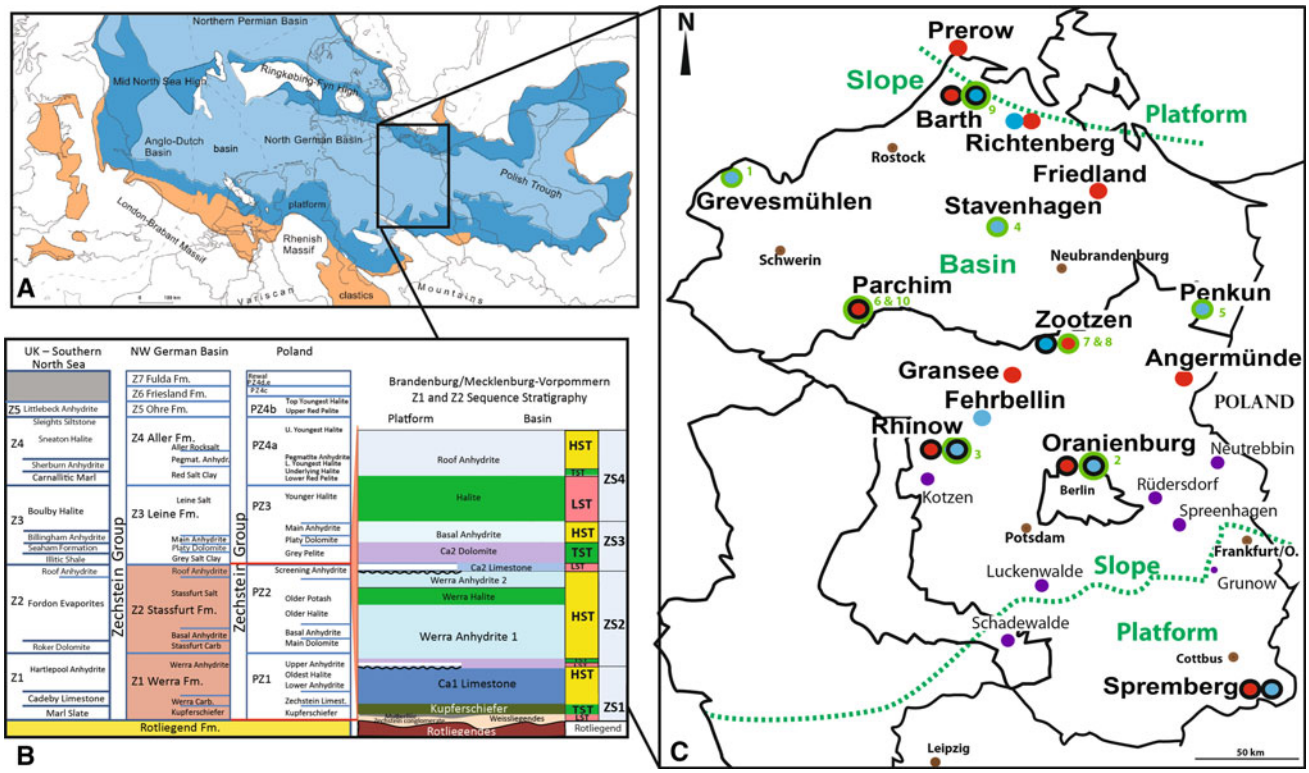

Fig. 1 **a** Paleogeography of the Z2 Southern Permian Basin illustrating platform and basin areas (modified from Geluk 2007). Inset shows location map of study area in C. **b** Stratigraphic terms of the Zechstein Formation-Group from United Kingdom (after Tucker 1991) to Germany (after Richter-Bernburg 1955) and Poland (after Wagner 2008). **c** The location map showing Zechstein 1 location of wells (*blue dot*), Zechstein Z2 wells (*red dots*) and Hartwig and Schulz (2010) wells (*purple dots*) used in the study of Brandenburg and Mecklenburg-Vorpommern. *Black circles* around *well dots* indicate wells used in cross sections (Figs. 2, 8). *Green circles* around *well dots* and *green numbers* indicate wells used in Table 1. *Green stippled lines* indicate boundaries of platform, slope and basin

thermal subsidence led to the formation of the Permian Basin (e.g., Ziegler 1990; Plein 1994; Geluk 2000). Volcanism in local pull-apart basins occurred throughout the basin in the Early Permian followed through middle Permian by deposition of up to 3 km thick sandstone succession of the Rotliegend in the basin. Thick volcanic deposits in the study area during Early Permian times created a regional high that persisted through deposition of the Rotliegend and Zechstein Groups (e.g., Ziegler 1990; Geluk 2007). Thermal contraction and subsidence coupled with a transgression from the Panthalassa Ocean in the north resulted in Upper Permian sedimentation of the Zechstein Group, comprising cyclic deposition of clastics, carbonates and evaporites (e.g., Ziegler 1990; Van Wees et al. 2000). Late Permian to Early Cretaceous salt mobilization and subsequent extensional reactivation of faults concluded the basin formation creating tectonic traps for prolific oil and gas reservoirs (e.g., Plein 1994; Strohmenger et al. 1996).

The Upper Permian Zechstein carbonates and evaporites are divided into seven cycles (Strohmenger et al. 1996; Käding 2000): Z1 = Werra; Z2 = Stassfurt; Z3 = Leine; Z4 = Aller; Z5 = Ohre; Z6 = Friesland; Z7 = Fulda (Fig. 1). Not all of these cycles are present across the Permian Basin (Fig. 1) but are developed in the study area (i.e., Northern German Zechstein basin). Designation of lithologic units in the Z1 and Z2 cycles are T1 for the Kupferschiefer, Ca1 for Werra carbonate, Ca2 for Stassfurt carbonate, A1 for Werra Anhydrite, and A2 for Basal Anhydrite. These lithologic units were subdivided into genetically linked sequences that are stacking into sequences and smaller-scale cycles. The whole Zechstein represents a second-order sequence (Tucker 1991) but smaller-scale cycles stack into third- to fifth-order sequences. Sequence stratigraphic subdivisions of the seven classic cycles followed by Tucker (1991) into seven sequences ZS1–ZS7 and eight sequences by Strohmenger et al. (1996), where Tucker interpreted all major anhydrite cycles deposited as lowstand systems tracts (LST) while Strohmenger et al. (1993, 1996) and Kaiser et al. (2003) interpreted the anhydrites to be part of the highstand systems tract (HST) and only the uppermost basinal anhydrite as part of the LST. This study uses and refines the large sequence stratigraphic framework produced over the years from these various authors, and adds a new, well-constrained correlation from shelf to basin showing the regional and stratigraphic variability of lithofacies types and their spatial arrangement in small- and medium-scale cycles. This level of information is essential to assess in detail shale-gas/oil and hybrid unconventional plays, especially where interfingering organic-rich mudstones and carbonates might present new exploration possibilities.

Previous studies

A comprehensive study of the unconventional reservoir potential and sequence stratigraphy of platform, slope and basinal facies of the Z1 and Z2 is lacking to date. Platform carbonates have been subject to many studies ranging from Poland to England (e.g., Tucker 1991; Strohmenger et al. 1996; Becker and Bechstädt 2006; Peryt et al. 2012; and many others) that concentrated mainly on the platform carbonates and evaporites. However, slope and basin facies did only just recently spike the author's interest because of their potential for shale gas and/or shale oil. Hartwig and Schulz (2010) evaluated the shale-gas potential of the organic-rich mudrocks in Z2 basinal and slope deposits of southern Brandenburg (see Fig. 1) addressing limited shale-gas potential due to low TOC and low formation thickness. Kupferschiefer geochemical papers are documented only from other parts of the Zechstein basin, such as Poland (Bechtel et al. 2000), Rheingraben (Bechtel and Püttmann 1997), Hessen Basin (Becker 2002; Becker and Bechstädt 2006). Paul (1986a, b, 1991, 2006) studied the Kupferschiefer sequence stratigraphy and facies in western Germany and compared to English Zechstein sequence described by Smith et al. (1986). Gerling et al. (1996a, b) evaluated source rock potential of the Ca2 from basin to lagoon and correlation to oils establishing the Ca2 as an actively generating hydrocarbon source rock in the states of Brandenburg, Mecklenburg-Vorpommern, Sachsen-Anhalt and Thüringen. Bechtel and Püttmann (1997), Bechtel et al. (2000), Kaiser et al. (2003), and Strohmenger et al. (1993, 1996) established a sequence stratigraphic model for the Stassfurt Formation. Petroleum potential of Polish Zechstein cores generated a slew of papers by the Polish Geological Survey. Some of these publications, namely Dyjaczynski et al. (2001), Kotarba and Wagner (2007), and Slowakiewicz and Mikolajewski (2009) and references therein established both the Kupferschiefer and Stassfurt basinal mudrocks to be actively generating source rocks for oil in low maturity settings.

Methods

This study is based on 17 cores that were described and selectively sampled at core repositories of geological surveys of Brandenburg and Mecklenburg-Vorpommern following a profile from the southern platform across the basin onto the northern shelf margin (Fig. 1). The depths ranged from 964 to 4,934 m. These cores were drilled during 1950–1970s as part of the research coring program that the former East German Erdgas Erdoel Gommern oil company conducted to evaluate the hydrocarbon potential in northern Germany.

Macroscopic core description, facies descriptions, thin-section petrography, and photomicroscopy were conducted on approximately 120 samples for the Z1 and Z2 intervals. Core material was partially incomplete and not always fully covering the full stratigraphic length of the drilled interval. These are marked in core descriptions. The cores were compared when possible to geophysical logs where logs were present or available. Thin-sections were examined to determine facies, grain types, and cementation. To evaluate the pore space on a micro-scale, selected samples were prepared with Ar-Ion milling technique (Loucks et al. 2012) or polished and examined under backscatter scanning electron microscope and environmental scanning electron microscope.

Selected samples were analyzed for TOC, thermal maturity, and significant minerals (Table 1). TOC analyses were conducted using a CHNOS Vario Elemental analyser by Elementar at the University of Potsdam. Geomark Laboratory, Houston, USA performed Rockeval pyrolyses and vitrinite reflectance measurements. Major minerals were determined with a Siemens Diffractometer D5005 in Bragg–Brentano reflection geometry. The diffractometer was equipped with a copper tube, a scintillation counter, automatical incident- and diffracted-beam soller slits and with a graphite secondary monochromator. The generator was set to 40 kV and 40 mA. All measurements were performed with sample rotating. Data were collected digitally from 3 to 70° 2θ using a step size of 0.02° 2θ and a count time of 4 s per step.

Archival data

The LBGR and LUNG (Geological Surveys of Brandenburg and Mecklenburg-Vorpommern, respectively) geological archives were used for gaining insight into reports generated by the former East German oil company, Erdgas Erdoel Gommern. These reports documented the stratigraphy, lithology, petrophysics, and geochemistry of selected intervals of the cores. Some of these data, such as porosity and permeability measurements, were used to gain insights into the drilled lithologies where core material was missing and is indicated in text.

Depositional environments, facies, and cyclicity

The Southern Permian Basin is characterized by several low-frequency and numerous high-frequency cycles related to sea-level fluctuations that are well documented and correlative across the basin (e.g., Peryt 1986; Paul 1991; Strohmenger et al. 1996). The underlying Rotliegend Group is composed of tan to red silt- and sandstones of fluvial and playa lake origin (e.g., Gebhardt et al. 1991;

Table 1 Rock-eval data, vitrinite reflectance and kerogen types from selected basinal and slope mudrocks across the basin for Zechstein 1 and 2 cycles. See Fig. 1 for location of numbered wells in green. Wells without numbers are from The Netherlands and England (i.e., OH-1-04, DT149/26-25-02)

Rock-eval data															Kerogen type	
Well number Fig. 1	Stratigraphy	Facies	Sample	depth	Carbonate (wt %)	TOC (wt %)	Tmax	S1	S2	PI	S3	HI	OI	Ro	Amorphous organic matter	liptinites
1	T1	Claystone	Gv-1-78-5	4,934.8		1.55	469	0.16	0.38	0.30	0.24	25	15	1.28		
	T1	Claystone	OH-1-02	3,177.9	43.37	0.61	440	0.17	0.66	0.20	0.23	108	38	0.76		
3	T1	Claystone	Rhi-2-9	4,217.9	26.69	0.84								2.01	86	7
4	T1	Calcareous laminated mudstone	Stav1h2-76-4	4,297.2	91.92	0.36								2.01	93	5
5	T1	Organic-rich mudrock	Pkn-1h2-71-5	4,172.4	18.00	6.04								2.22	93	4
2	Ca1	Calcareous mudstone	Obl-68-8	3,496.2		0.86	451	0.20	0.40	0.33	0.13	47	15	0.96		
6	Ca2	Laminated calcareous mudstone	Pal-68-28	4,635.5		0.55	520	0.05	0.29	0.15	0.30	53	55	2.20		
	Ca2	Laminated calcareous mudstone	OH-1-07	3,093.5	89.01	0.45	440	0.62	1.03	0.38	0.65	229	144	0.76		
	Ca2	Laminated calcareous mudstone	OH-1-04	3,131.8	43.20	0.15	496	0.17	0.27	0.39	0.19	180	127	1.77		
	Ca2	Laminated calcareous mudstone	DT149/26-25-02	1,839.2	96.49	0.31	446	0.21	0.62	0.25	0.17	200	55	0.87		
9	Ca2	Laminated dolo-mudstone slope	Barth-1-63-2	2,814.2	83.38	0.32								0.92	86	12
10	Ca2	Laminated bituminous mudstone	Pa1-68-25	4,636.9	81.31	0.45								3.84	90	6

Gaupp et al. 2000; Legler et al. 2005). Related to the ensuing transgression of the basin from the northwest the Kupferschiefer (T1) with blackish to dark-greyish colored, organic- and clay-rich shale was deposited. Overlying the shale is the Werra carbonate (Ca1) followed by dolomite and the Werra Anhydrite. The limestones and dolomites of the Stassfurt carbonate (Ca2) on the shelf and the Stinkschiefer ("smelly shale") in the basin were overlain by the Stassfurt anhydrite completing the Z2 cycle in the Permian Basin. Although major sequence boundaries can be correlated across the basin, facies and variations in cycle thickness are predominant in subbasin-depressions and subbasin-highs related to paleogeographic variations rooted in Middle Permian Rotliegend time. For example, the study area is underlain by a volcanic plateau that spread across the area and created a high during subsequent fluvial Rotliegendes and Zechstein deposition (see Geluk 2005; Scheck-Wenderoth and Lamarche 2005; Peryt et al. 2010). This intrabasinal high seemed to have been responsible for subsequent facies differentiation in overlying formations ranging from Upper Permian to Cretaceous.

Three major depositional domains, platform, slope, and basin, can be differentiated in the Z1 and Z2 Zechstein units from the platform in the north across the basin to the platform in the south (Fig. 1).

Zechstein 1

The Zechstein 1 represents a complete transgressive to regressive cycle. In detail this sequence is composed of two higher-frequency sequences that exhibit different character depending on the position of the section in the basin (Fig. 2). In the first sequence, ZSI-1, organic-rich shales and marine carbonates dominate, shallowing upward into grain-dominated carbonate facies. The second sequence ZSI-2 grades from sabkha and tidal flat facies into dolomitized limestones and anhydrite (Fig. 2). In contrast to the basin and swell facies of the western part of the Permian Basin (e.g., Paul 1986a, b) the study area of Brandenburg and Mecklenburg/Vorpommern does not exhibit a fragmented paleogeography or reefal structures in the Z1. In fact, the Z1 depositional profile does not indicate much facies variability from slope to basin (Fig. 2). Strohmenger et al. (1996) and Becker and Bechstädt (2006) proposed sequence stratigraphic subdivisions of two 3rd-order sequences for the Z1 cycle: the ZS1 and ZS2 sequences, which correspond to this paper's two sequences, ZSI-1 and ZS1-2. However, a major exposure surface between the two sequences, as indicated by Strohmenger et al. (1996) has not been observed, which agrees with Becker and Bechstädt's findings of this surface being restricted to intrabasinal highs. New age dates (e.g., Menning et al. 2005; Szurlies 2013), however, suggest shorter duration and therefore higher-frequency order for these two sequences of probable 4th-order duration. Szurlies (2013) estimated a duration of up to 3.5 m.y. for the whole Zechstein with the Z1 and Z2 cycles lasting about 2 m.y. According to sequence stratigraphic convention (e.g., Vail et al. 1977; Haq et al. 1988) a third-order cyclicity might be assigned to these two cycles instead of second-order cycle as suggested by Strohmenger et al. (1996). Six facies types were identified that are stacking into two sequences. The ZSI-1 sequence is subdivided into three smaller-scale cycles ZC1-1 through ZC1-3 (Fig. 2). These sequence subdivisions were also recognized by Strohmenger et al. (1993, 1996). The first sequence is dominated by four distinct facies types illustrating the transition from a fluvial to playa lake dominated environment of the underlying Rotliegend Group to marine transgressive facies of the Zechstein ranging from clay-rich mudstones to carbonate-dominated facies (facies types ZF1-1 to ZF1-4). The second sequence, ZS1-2, is dominated by evaporite facies expressed in dolo-mudstones and anhydrites (facies types ZF1-5 and ZF1-6) and contains one cycle ZC1-4. The thickness of the Z1 carbonates and mudrocks (not including the anhydrite and salt) varies from fairly uniform in the basin of <10 to 15–20 m on the slope, and >20 m on the platform (Fig. 2). Porosity ranges from 1 to 6 % and permeabilities <0.001 in mudrocks to 1 mD in carbonates. Depositional facies are described below to identify stacking patterns that can be traced into genetically linked units. The facies are varying across the basin from mudrocks to evaporites and present interfingering source rocks, seals, and reservoirs, as discussed below.

Zechstein 1 facies types

ZF1-1: calcareous laminated organic-rich mudrock This heavily compacted facies is composed of 0.1–1.2 m thick, laminated, organic-rich shales that contain grains composed of apatite, albite, quartz, biotite, pyrite, and muscovite amongst layers of clay, organics, and calcite crystals (Figs. 3, 4). Sedimentary structures of these laminated shales include rare burrows and cross-laminations that are predominantly located in slope areas. The shales exhibit low porosity mainly in interparticle pores and in micro- and nano-pores within the organic material. Bulk porosity is typical <2 % and permeability <0.001 mD. This facies can be traced across the Southern and Northern Permian basins and was deposited in response to flooding of the Permian Basin from the northwest (e.g., Paul 1986a, b; Ziegler 1990; Kopp et al. 2006; Geluk 2007) from shelf to basin in fairly uniform thickness of 0.5 m in most sections (Fig. 2). It is one of the prolific source rocks in the Permian Basin for many of the overlying reservoirs stretching from Poland (e.g., Bechtel et al. 2000) to England with TOC content

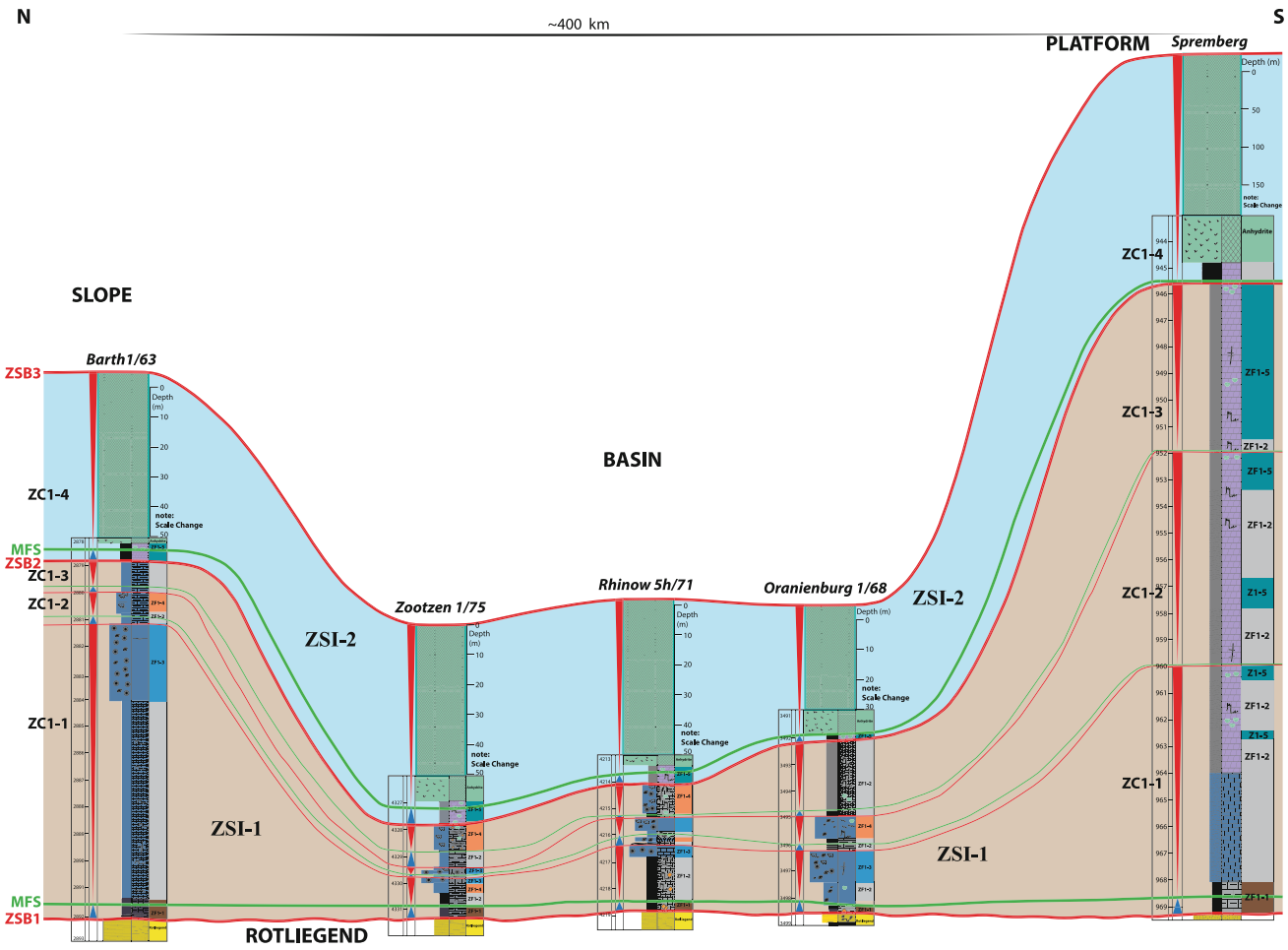

Fig. 2 Cross section from north to south platform across the basin showing Z1 sequences, cycles, and lithology. Two sequences ZSI-1 and ZSI-2 showing shallowing-upward patterns on platform, slope and basin. These sequences compare to Strohmenger et al. (1996) sequences. ZSB3 is sequence boundary on top of Lower Werra Anhydrite. The Na1 salt and A1b Upper anhydrites were not logged in this study. Not to horizontal scale. Note scale change in last sequence (anhydrite)

ranging from 1.6 to 6 % and maturities ranging from oil window on the slope and platform to overmature in the basinal area of the study area (Table 1).

ZF1-2: calcareous laminated mudstone Main constituents of mudstones and laminated mudstones are composed of layers of micrite, calcite, clay, and organic material. The mudstones occur at the bottom of each ZF1 sequence but above the Kupferschiefer (Figs. 3, 4). This facies gradually overlays the organic-rich shales with dark-grey laminated to massive, calcitic mudstones. Bioturbation is present in some of the samples but rare. High-amplitude and micro stylolites are common in this facies. Cross-stratification in samples from the slope indicate current action. TOC content of this calcareous facies is <0.5 % (Table 1).

ZF1-3: calcareous oncoid peloid intraclast wacke-/packstone Slope and basin environments are characterized by coated grain, oncoid, peloidal, intraclast wacke- to packstones overlying laminated mudstones (Fig. 3). Main constituents in a predominantly micritic matrix are oncoids, peloids, intraclasts, skeletal grains, and diverse silt-sized grains. The matrix is micritic but sparite is present between some of the oncoids and peloids. Where oncoids are cemented, they appear as interclasts in micritic matrix. Oncoid size ranges from micrometer to 2 mm. Porosity is present in rare intra- and interparticle pores.

ZF1-4: calcareous thrombolite wackestone to bindstone Microbially bound mud- and wackestones are abundant in the slope and basin environment of the Z1 rocks. This facies is characterized by micritic matrix with clotted microbial fabrics (mesoclots sensu Kennard and James 1986). Cauliflower shaped clumps of microbial microstructures form mesoclots that are bound by microbial mats (Fig. 3). This framework is due to in situ calcification that is creating a rigid framework (Kennard and

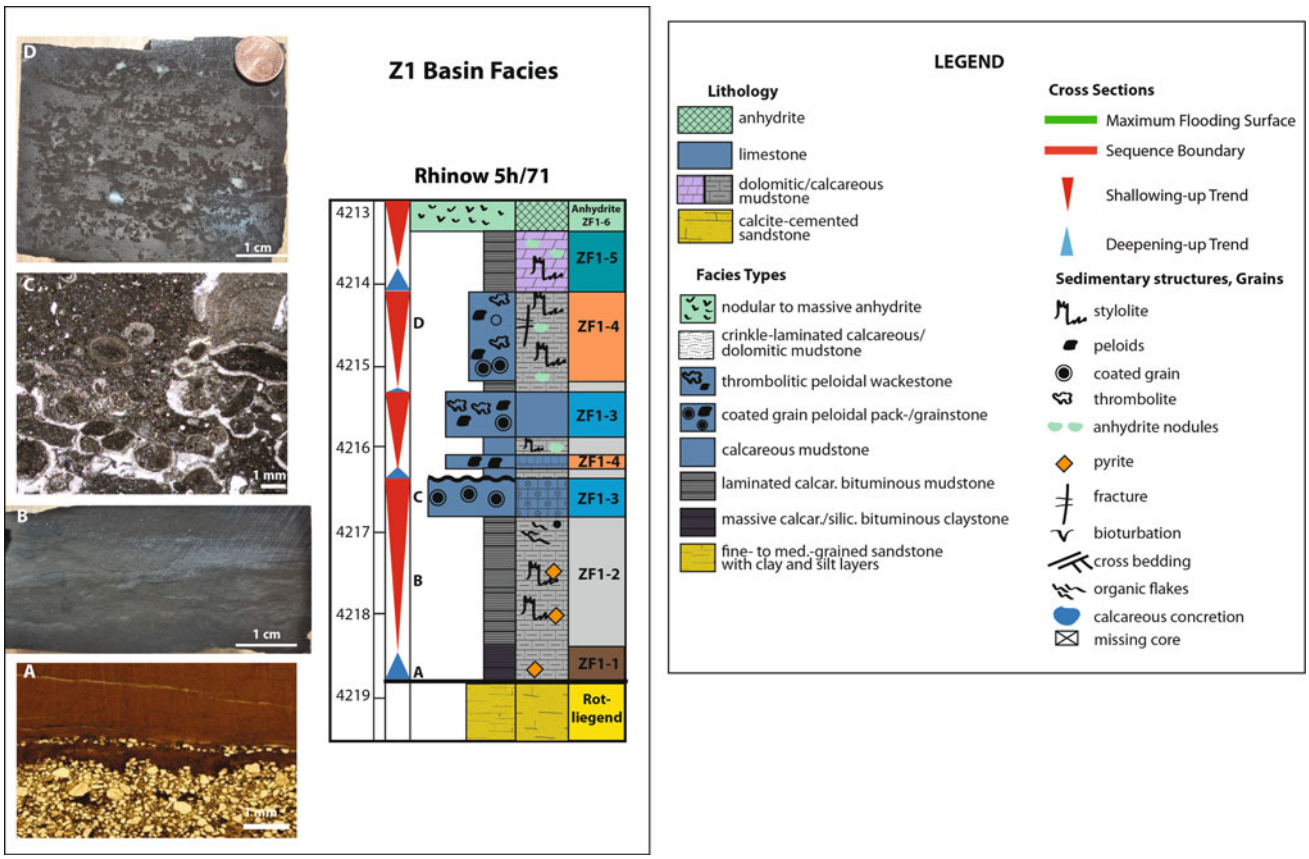

Fig. 3 Thin-section photomicrographs and whole core examples of Z1 basinal facies of Rhinow 5h/71 well: **a** Facies type ZF1-1—Core Kupferschiefer/Rotliegend boundary showing contact of sandstone to claystone. **b** Facies type ZF1-2—laminated bioturbated mudstone; **c** Facies type ZF1-3—Coated-grain peloid packstone; **d** Facies type ZF1-4—thrombolitic, calcareous wacke- to packstone. Legend is applicable to Figs. 3–8

James 1986). The thrombolite facies occurs associated with facies ZF1-3 or overlies the oncoid facies. Its porosity occurs mainly in moldic and intercrystalline pores but is usually below 6 %.

ZF1-5: dolo-mudstones The top of the platform to basin Z1 cycle is characterized by structureless carbonate mudstones that are often dolomitized (Figs. 3, 4). These mudstones contain anhydrite nodules and anhydrite crystals due to proximity of overlying anhydrite. Dolomite/anhydrite dominated facies is prevalent on the top of the basinal facies as <1 m thick dolo-mudstone with anhydrite nodules.

ZF1-6: anhydrite facies The transition to the Werra Anhydrite is gradual from interbedded dolomite and anhydrite grading into mosaic and massive anhydrite within <1 m (Fig. 4). The Z1 anhydrite is divided into a lower and an upper anhydrite package. In some areas the anhydrite units are intercalated with salt. The anhydrite package is thickest on the slope and platform but thinner in the basin. Frequently, this anhydrite package is intercalated with salt, called the Na1, within the Werra stratigraphic section.

Interpretation Z1 stacking patterns and sequence stratigraphic framework

Above the Rotliegend unconformity the transgressive systems tract (TST) of the Z1-1 cycle is expressed as marine sandstones, conglomerate and organic-rich mudrocks. The mudrocks or shales were deposited under anoxic to disoxic conditions below a stratified water column as evidenced by the almost complete absence of fossils, high amount of preserved organics, and botryoidal pyrite (see also Paul (2006) for genesis of Kupferschiefer). Laminations of more calcite-rich and clay-rich layers indicate suspension fallout of very fine-grained clastic and organic-rich material. Bioturbated units represent times of more oxygenated conditions related to small-scale sea-level fluctuations or episodes of increased freshwater runoff which would temporarily increase oxygenation. Following the widespread transgression were an increase in sea level that established more normal marine conditions in the basin and

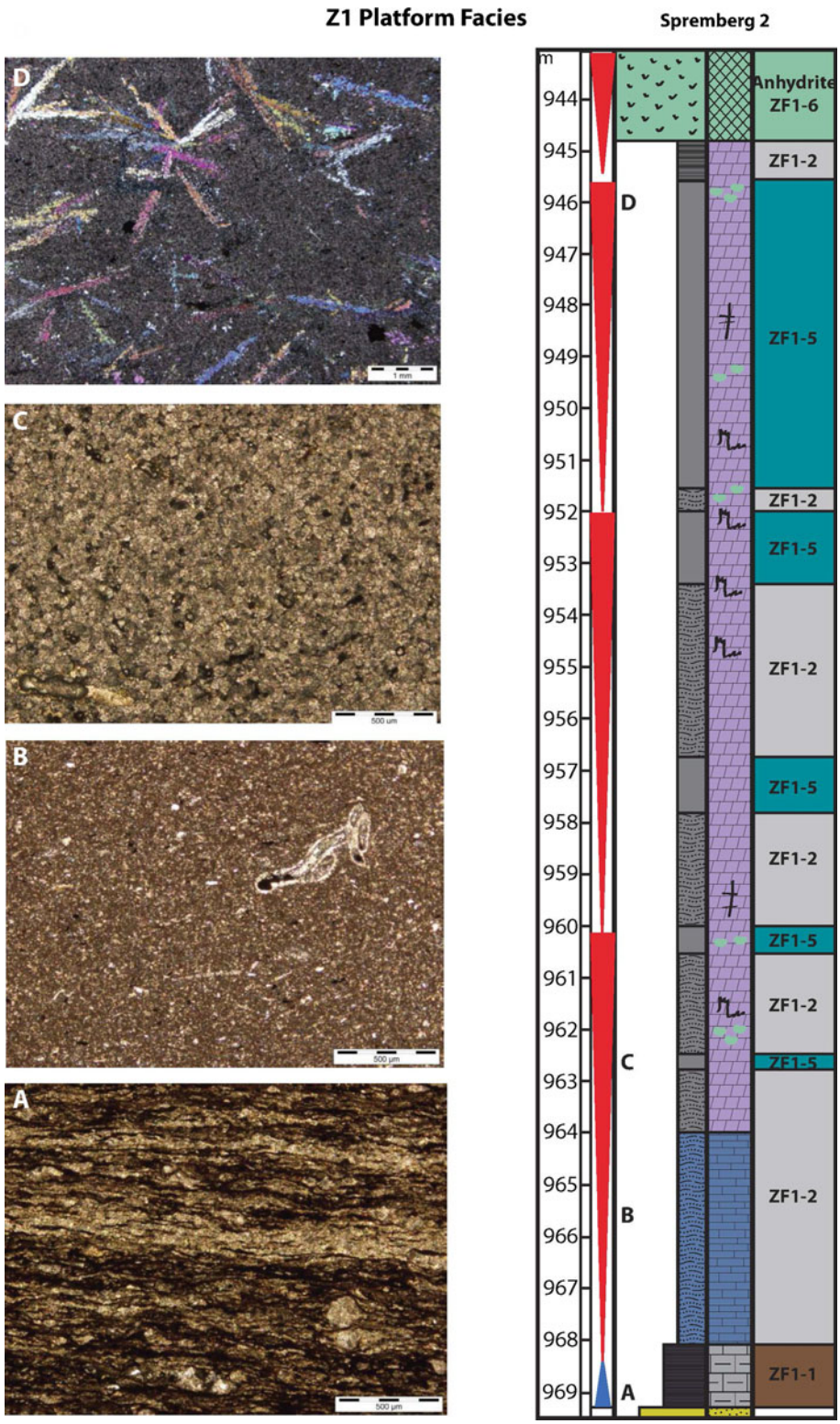

Fig. 4 Z1 platform facies and core log of Spremberg 2 well: thin-section photomicrographs of the platform showing laminated organic-rich mudstone of facies type ZF1-1 (**a**); calcareous laminated mudstone of facies type ZF1-2 (**b**); dolomitic mudstones of facies type ZF1-5 (**c**, **d**); and dolomite with anhydrite crystals (**d**). See Fig. 3 for legend

evaporitic conditions on the platform (Ziegler 1990; Van Wees et al. 2000). Above an exposure surface on the shelf and parts of the basin the second Z1-2 sequence indicated a change to more arid conditions resulting in thick anhydrite and salt deposits.

Stacking-patterns and facies development of each of the two sequences ZSI-1 and ZSI-2 illustrate the overall regressive nature and interfingering of mudrocks and carbonates in the basin and along the slope. ZSI-1 is divided into three smaller-scale cycles ZC1-1, ZC1-2, and ZC1-3.

This subdivision was also recognized by Becker and Bechstädt (2006) and Strohmenger et al. (1996). Each cycle is shallowing-upward and capped by oncoid packstones or thrombolite wackestones becoming progressively thinner toward the top of ZSI-1. The second sequence ZSI-2 is dominated by transgressive organic-rich dolomites and anhydrite composing the HST.

The TST of each sequence is composed of organic-rich mudrocks and mudstones (Figs. 2, 3). In the ZSI-1 sequence these mudrocks are representing the Kupferschiefer equivalent, an organic-rich mudrock of ZF1-1 facies with TOCs reaching 6 % in the study area (Table 1). Platform mudrocks are slightly more calcitic but also contain high amounts of organics evidenced by a current value of 4.5 % TOC. Three smaller-scale cycles were reported by other authors (e.g., Rentzsch 1965; Gerlach and Knitzschke 1978; Paul 2006) within the Kupferschiefer organic mudrocks. However, these three cycles were not observed in the study area and are mostly present on the platform. The maximum flooding surface is expressed within the organic-rich mudrocks. The HST in cycle ZSI-2 is typically composed of laminated mudstone of facies type ZF1-2 above the organic-rich mudstones. In the basin, these are sharply overlain by oncoid-peloid packstones and grainstones of facies type ZF1-3 indicating shallowing and wave-base influence. Although, Füchtbauer (1968) interpreted oncoids for the Zechstein in northern Germany to be of subtidal origin deposited in relative quiet water depths larger than 30 m, the association of oncoids, aggregate grains, and ooids of varying sizes supports deposition influenced by some current/wave activity. These basinal oncoid packstones interfinger and are overlain by thrombolite wackestones of facies ZF1-4. Thrombolites suggest fixation of the sediment by microbial interaction as evidenced by the clotted nature (e.g., Kennard and James 1986; Fig. 3). Thrombolite and oncoid grainstone facies compose the tops of each cycle. In some cores these facies also exhibit exposure surfaces and karst dissolution features related to subaerial exposure. Platform cycles above the organic-rich shale are dominated by dolomitized mudstones of alternating ZF1-2 and ZF1-5 facies that reflect subtidal to tidal-flat environments. Scarce foraminifera are present in the massive lime mudstone overlying the organic-rich mudstone but most platform facies are devoid of organisms. Most depositional textures are destroyed higher up in the section due to pervasive dolomitization. Towards the top of each platform cycle anhydrite is increasing in form of nodules and crystals either caused syndepositionally or later diagenetically.

The second sequence, ZSI-2, of the Z1 cycle is characterized by dolomitized limestones and mudstones with anhydrite nodules and crystals indicating a shallowing from subtidal to tidal flat conditions, as well as an increase in evaporitic conditions (Fig. 2). Basin and platform show similar facies in this second cycle indicating an overall shallowing and increase in salinity and likely evaporitic conditions across the basin (e.g., Richter-Bernburg 1985; Becker and Bechstädt 2006). This second sequence encompasses the thick section of Werra Anhydrite that dominated the late HST with thick deposits on the slope and platform but thinner deposits in the basin. Continued subsidence and accommodation space facilitated deposition of basinal anhydrite during highstand conditions completing the Z1 sequence. The top of this second sequence, ZSB3 is characterized by a widespread exposure surface and evaporite karst (e.g., Steinhoff and Strohmenger 1996; Strohmenger et al. 1996; Leyrer et al. 1999). Exposure surfaces and karst features were recognized in cores on the platform and shallow slope; the ZSB3 in the basin is distinguished by an abrupt transition from anhydrite to calcareous mudstone that is correlating to the exposure event on the platform.

Zechstein 2

Z2 cycle, ranging in thickness from 15 to 20 m in the basin and 20 to 30 m on the slope and platform, also comprises a series of stacked cycles. In contrast to the Z1 sequence significant differences in morphology from platform to basin were established by differential compaction and establishment of thick anhydrite- and salt-dominated, wall-like structures which separate the marginal platform from slope and basinal deposits (e.g., Richter-Bernburg 1985; Strohmenger et al. 1996). The Z2 sequence rests unconformably above the Werra Anhydrite. Dolomitized, laminated, mud- and wackestone dominate the facies in the platform area whereas the basin exhibits organic-rich laminated mudstone and calcareous and dolomitized mudstones. Most of the marginal deposits of the Spremberg area are characterized by micritic carbonates that were dolomitized starting very early in the post-depositional history, organized in cycles shallowing-upward into tidal-flat strata with typical features like bird's-eye structures and nodular anhydrite typical of coastal sabkha environments. This sequence is in turn overlain by the Basal Anhydrite that blanketed and filled in the depositional geometry across the basin.

Zechstein 2 facies types

ZF2-1: laminated dolo/lime mudstone facies The laminated mudstone facies is the dominant facies of the Z2 basinal and slope carbonate section and characterized by mm- to cm-thick layers of calcite, dolomitized calcite, dolomite, and mm-thick, dark layers composed of finely crystalline dolomite, organics, clay, and silt (Fig. 5).

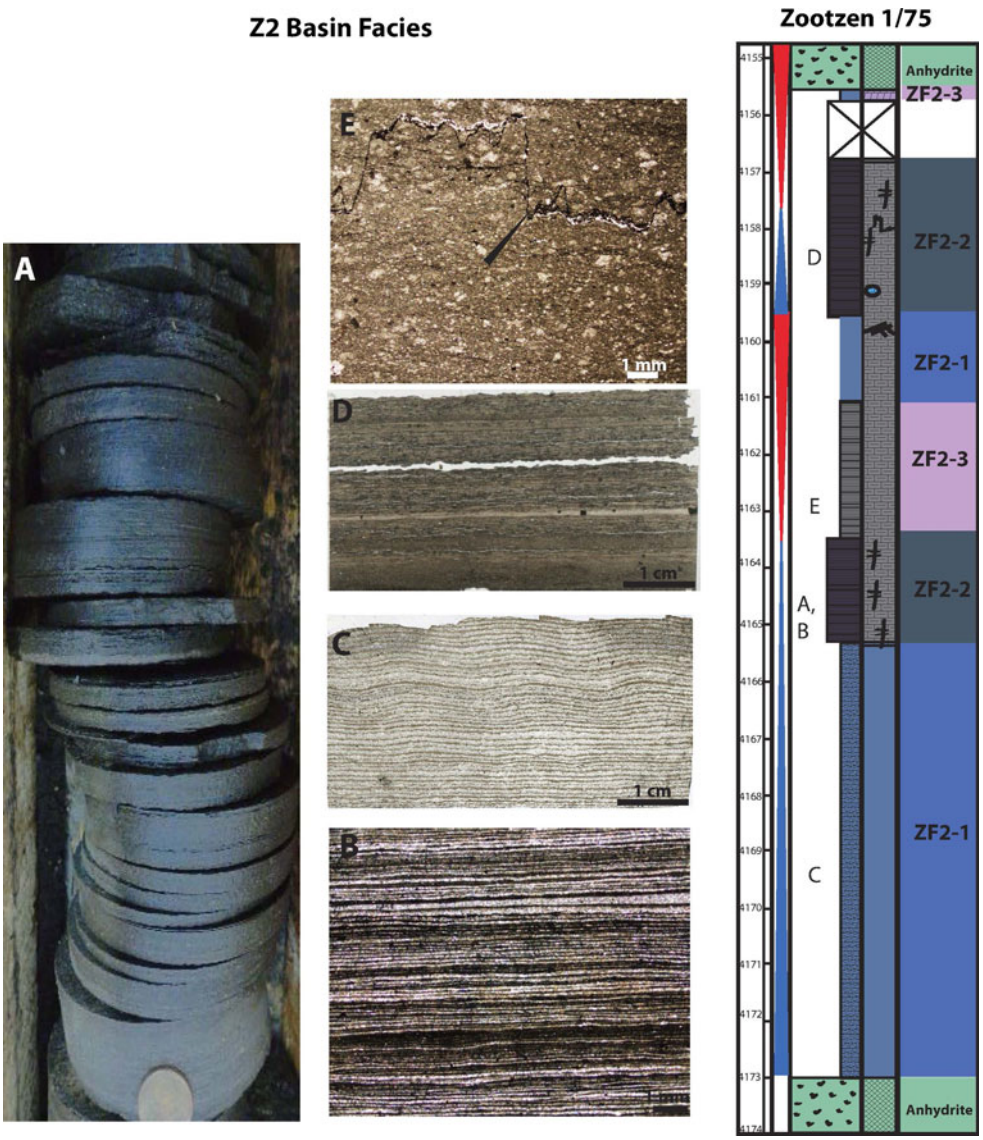

Fig. 5 Z2 basinal facies and core log and thin-section of Zootzen 1/75 well: core photograph of bituminous laminated calcareous mudstone (**a**); thin-section photomicrograph of bituminous laminated calcareous mudstone (**b**); Crinkled varve-laminated mudstone showing alternate layers of calcite and clay, silt, and organics (**c**); ZF2-3 facies showing dolo-mudstone with layer of dolomitized mudstone, dolomite and clay. Black specs are pyrite (**d**); Skeletal wackestone of facies ZF2-3 showing high-amplitude stylolite filled with bitumen and clay (*arrow*). See Fig. 3 for legend

Stylolites along bed boundaries are commonly filled with bitumen, clay and silt (Fig. 5). These stylolites also cross-cut some of the laminae. This facies is more prevalent on the slope and shallower parts of the basin and towards the top of cycles. Where this facies is dolomitized within close range of any of the Werra or Basal Anhydrite, anhydrite nodules are present.

ZF2-1A: crinkled varve-laminated mudstone facies The varve-like appearance in these calcitic mudstones ranges from perfectly horizontal laminae to crinkled laminae (Figs. 5, 6). The laminae consist of wavy layers of light-colored calcite and dark layers composed of fine-crystalline dolomite, clay, bitumen, and silt. The lighter colored layers are cm- to mm-thick and thicker where convex upward, whereas the dark layers are μm- to mm-thick laminae. The crinkly varve-laminated mudstone facies occurs only in the basin and slope environments. Overall thickness of the crinkled varve laminite facies is 4–6 m in the basin but 10+ meters on the slope; each crinkled bed is cm to dm thick intercalated between laminated beds that are also cm to dm thick (Fig. 5).

ZF2-2: organic-rich laminated mudstones facies The organic-rich laminated mudstone facies is dominating the basinal and slope section of the Z2 cycle. Millimeter- to centimeter-thick laminae consist of mm- to cm-thick calcite layers and mm-thick layers of organics, clay, silt, and pyrite (Fig. 5). Some intercrystalline pores are filled with bitumen. Where this section is deeply buried and over-mature the carbonates exhibit a dark brown to black fissile appearance and hydrocarbon smell (e.g., Stinkschiefer facies) related to deep burial and maturation (Fig. 5). Within slope and basin sections, this facies contains thin-

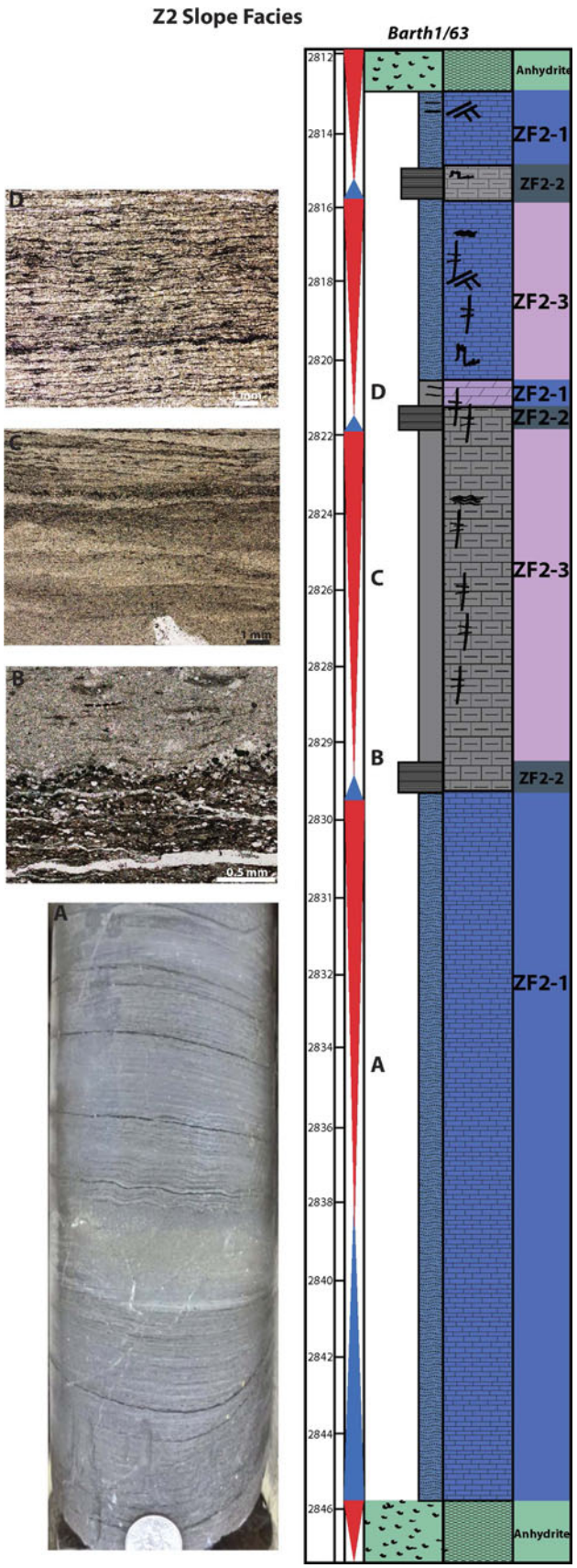

◀ **Fig. 6** Z2 slope core and thin-section photomicrographs of Barth 1/63 well showing crinkle varve-laminated bedding (**a**), calci-turbidite representing coarser layer on top of organic-rich mudstone (bottom layer) (**b**), cross-bedding in laminated mudstone (**c**), and laminated mudstones of Z2-1 facies type (**d**). See Fig. 3 for legend

bedded turbidites composed of fine-grained lime-mud (Fig. 6).

ZF2-3: dolomitized/calcareous-mudstone facies This mudstone facies is characterized by dolomitized mudstones, with fine to medium crystal size. When dolomitized, the depositional fabric has been completely replaced. This facies, macroscopically, comprises massive beds with either cryptic laminations or traces of bioturbation. Occasionally, this facies is characterized by high amounts of porosity and by fractures filled by calcite cements. This facies is predominant on the platform but also present at cycle tops within the slope and basin (Fig. 7). In basinal settings this facies appears to be massive and contains fossil debris, stylolites, cross-bedding and bioturbation (Fig. 6). The dolomite fabric is tight with scarce porosity in intercrystalline pores. In some areas of the basin these mudstones show cross-bedding indicating some current action in the basin and along the slope (Fig. 6).

ZF2-4: fenestral fabric dolo-mudstone facies This facies composes the uppermost carbonate facies of each individual platform cycle and is characterized by finely crystalline dolomite, with laminations, likely related to microbial activity, fenestral fabrics and local anhydrite nodules (Fig. 7). As in Facies ZF2-3, the dolomitization has completely replaced the depositional fabric, precluding more specific characterization. This facies exhibits higher porosity in the fenestral fabrics and intercrystalline porosity when dolomitized. A more detailed diagenetic study would be required to assess in more detail the relationships between depositional fabrics, dolomitization events, dissolution and fracturing as well as later burial features. Such a study is currently underway.

Interpretation of Z2 stacking patterns and sequence stratigraphic framework

In contrast to the Z1 sequences, where facies changes are lithologically pronounced, changing from a more argillaceous to calcite- and evaporite-dominated lithologies, the Z2 facies are characterized by low to absent clay and complete dolomitization of the primary carbonate. These features are compatible with a stronger evaporitic regime in response to an overall 2nd-order fall in sea level towards the end of the Permian and resulting change in sea-water chemistry (e.g., Richter-Bernburg 1985; Strohmenger et al.

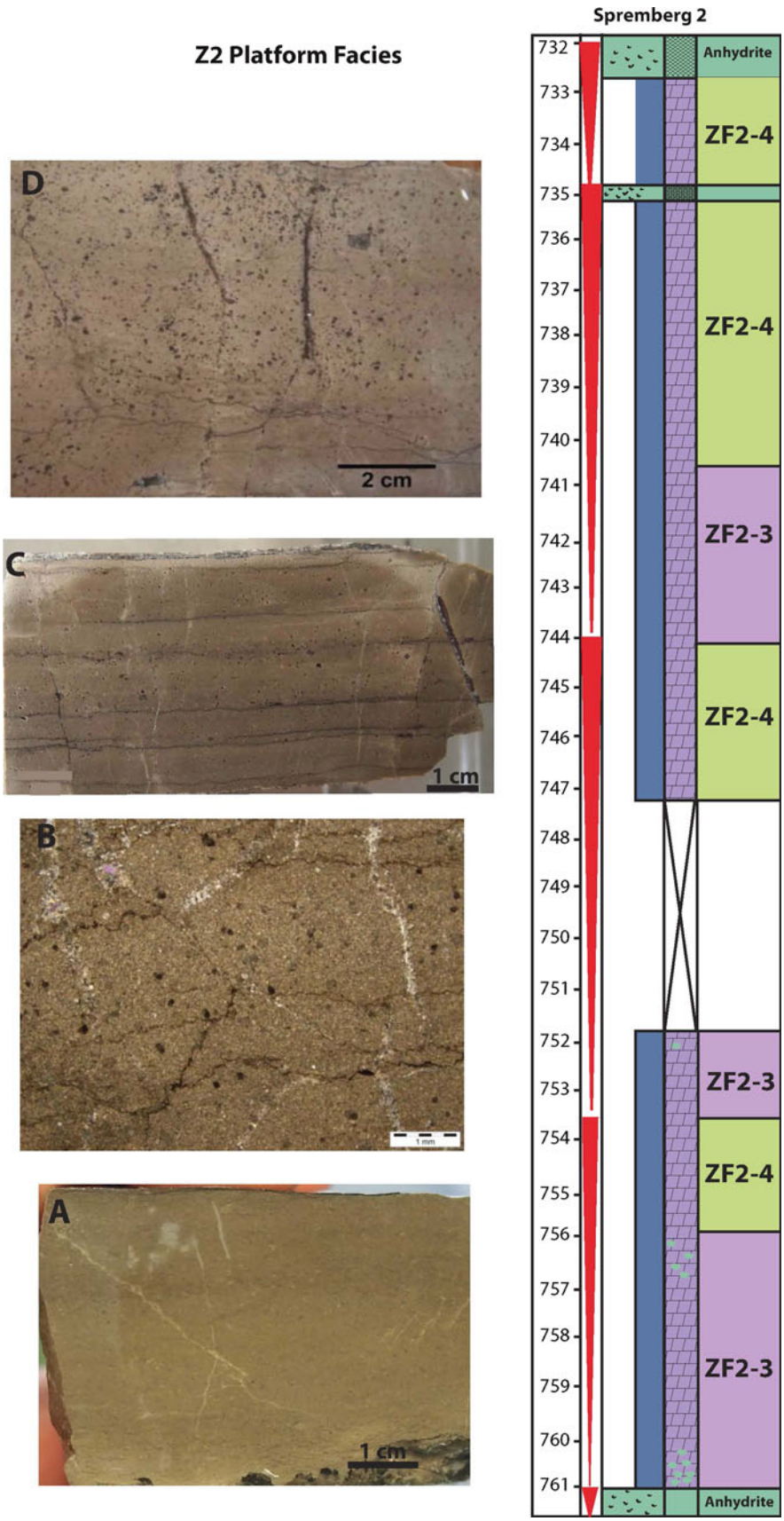

Fig. 7 Z2 platform core and thin-section photomicrographs of Spremberg 2 well showing dolo-mudstone facies ZF2-3 and ZF2-4. ZF2-3 is composed of tight dolo-mudstones (**a**, **b**) with sparse depositional textures. The ZF2-4 facies exhibits laminations with fenestrae fabrics (**c**) and rootlets (**d**). See Fig. 3 for legend

1996; Leyrer et al. 1999). This change from the Z1 to the Z2 cycle is probably related to climatic change from wet to dryer conditions towards the end of the Permian (Roscher and Schneider 2006), but could also be seen in the context of mega-monsoon related changes in precipitation versus evaporation typical of the Pangean continent (Mutti and Weissert 1995). Three medium-scale sequences, ZSII-1, ZSII-2, and ZSII-3, and four higher-frequency cycles, were identified in basin to platform sections with pronounced facies differences in each sequence (Fig. 8). These cycles are in contrast to Strohmenger et al. (1996) and Kaiser et al. (2003) who grouped the four higher-frequency cycles into two sequences of the Z2 cycle.

Above the Werra Anhydrite, which forms a major sequence boundary (ZSB3) (e.g., Strohmenger et al. 1993; Kaiser et al. 2003; Fig. 8) that exhibits karst solution features on the platform (Kaiser et al. 2003), occurs a mostly calcitic mudstone facies (ZF2-1) in the basin. While on the platform the maximum flooding surface lies directly on the Werra Anhydrite (e.g., Steinhoff and Strohmenger 1996), in the basin the TST is expressed as a sharp boundary between massive anhydrite and calcitic mudstone with abundant anhydrite nodules. These mudstones represent the TST of ZSII-1 (see also Strohmenger et al. 1996) and grade upwards into laminated lime mudstones and crinkled varve-laminated mudstones representing the HST on the slope and basin. According to Richter-Bernburg (1985) and analogues from the Permian Castile Formation in West Texas (e.g., Anderson et al. 1972) these varve-like laminated mudstones were caused by cyclical variations in salinity during evaporation in the basin and slope. The crinkled laminated mudstones above ZSB3 might have originally been composed of anhydrite but were later diagenetically modified to calcitic mudstone. These laminae can be correlated across the Permian Basin indicating basin-wide cyclical changes in salinity probably related to climatic fluctuations (e.g., Richter-Bernburg 1985). Basinal to slope environments are typical for this facies that does not occur on the platform (Peryt et al. 1993; Anderson et al. 1972). An abrupt change to organic-rich dolomitized mudstone lithology of facies type ZF2-2 indicates deepening and/or restriction in the basin and deposition of second cycle ZSII-2. Two higher-frequency cycles dominated by organic-rich mudstones and dolomites (Stinkschiefer, Stinkkalk) characterize this second cycle in the basin. Organic-rich mudstones are overlain by laminated calcareous mudstones of Facies ZF2-3. This facies also contains turbidite intercalations with fine-grained carbonate mud or bioclastic debris flows transported from the platforms. This facies is then overlain by a dolomitic, microbial-laminated mudstone that forms the cycle top of each stacking packet. The third sequence contains organic-rich mudstones that are abruptly overlain by dolomitized laminated mudstones and evaporites in the basin indicated shallowing and change to more evaporitic environments. The Z2 platform facies are organized in stacked cycle sets, with the ZF2-3 dolo-mudstone facies at the base, grading upward into the ZF2-4 laminated fenestral fabric dolo-mudstone facies, likely recording shallowing-upward cycles of the HST. At the top of the Z2 cycle, the ZF2-3 dolo-mudstone facies is directly overlain by evaporites reflecting an abrupt shift from subtidal to supratidal environment as seen in the basin. The depositional characteristics, despite the strong dolomitization overprint, are compatible with deposition on a shallow, low-energy shelf, periodically exposed to inter- to supra-tidal conditions. At the end of the Z2, the deposition of the Basal Anhydrite records the onset of a widespread evaporitic phase.

Distribution of facies and depositional geometries

Basin geometry and paleotopography (depositional relief) determine the detailed distribution of the different facies (Fig. 2). In the study area, the underlying Rotliegend Group is composed of mainly fluvial sediments compared to more salt-pan sediments in the basins towards the east and west (e.g., Poland, northwest Germany, Netherlands; Leyrer et al. 1999; Geluk 2005, 2007). This difference is related to a previous high that was caused by lower Permian volcanics that spread across the Brandenburg and Mecklenburg-Vorpommern area. As soon as marine conditions were established from a transgression from the north (Ziegler 1990) minimum facies and thickness variations from platform to basin suggests that bathymetric differences were not extensive during Z1 mudrock and carbonate deposition in the study area (Fig. 2). Thickness of the T1 mudrock facies (Kupferschiefer) is fairly thin across the basin ranging from 30 cm to 1 m (0.4 m average) filling in the relief of the underlying Rotliegendes Group. The overlying carbonate facies of the Ca1 exhibits similar facies associations across slope to basin with calcareous mudstones, wackestones and oncoidal and thrombolytic packstones except in low-lying areas on the platform such as the lagoon of the Spremberg Structure. Here the facies is mostly micritic, suggesting deposition in a semi-restricted lagoon, repeatedly shallowing upward into sabkha environments with dolomite and anhydrite nodules enhancing the depositional profile to double the thickness as the basin. The slope environments also show increased thickness yet similar stacking of grain-dominated and mud-dominated fabrics as the basin. The cyclicity is expressed in the rest of the basin by the repeated superposition of oncoid–peloidal and thrombolytic packstones, wacke- and mudstones, indicating fluctuations of wave base in basin and slope environments. An interpretation of in situ deposition of the pack- and grainstones is favored

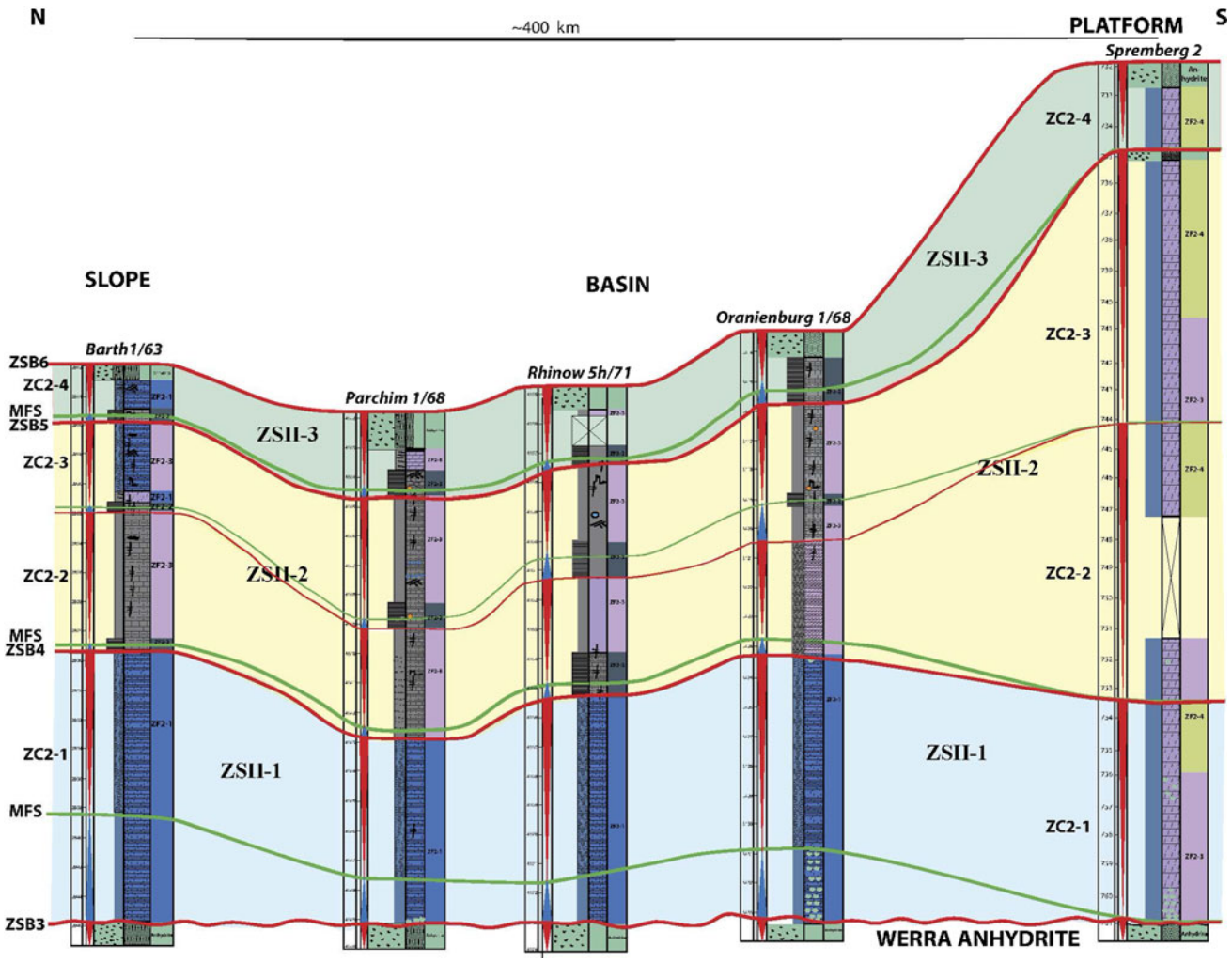

Fig. 8 Z2 cross section from north to south platform showing cyclicity and facies variations in cores. Three sequences, ZSII-1, ZSII-2, and ZSII-3, are correlated from basin to platform. ZSII-1 and ZSII-2 sequences show deepening upward patterns whereas ZSII-3 showing progressively shallowing-upward pattern. The upper sequence, ZSII-3 is culminating in thick anhydrite and salt deposits of the Basal Anhydrite and Stassfurt salt illustrated in *light blue* to top of section. Not to horizontal scale. See Fig. 3 for legend

because of the lack of sedimentological evidence indicating mass-flows deposited in the basin as might have been possible from platform-rimmed carbonate platforms (e.g., Playton and Kerans 2002; Janson et al. 2012). Similar deposits were also observed in Poland and interpreted as in situ deposited basinal facies (e.g., Peryt et al. 2010, 2012). These data, together with the minimal differentiation of facies across the depositional domains, indicate that in the paleotopographic relief during the deposition of the Z1 unit of mudrocks and carbonate was fairly low. This geometrical configuration suggests that the vertical stacking of mudrocks and overlying, partially interfingering carbonates can be traced laterally across the basin. Only during anhydrite and salt deposition of the Werra Anhydrite, a pronounced platform-rimming basin topography was established (Richter-Bernburg 1985; Strohmenger et al. 1996).

Z2 stacking-patterns and facies commenced above the karsted Werra Anhydrite unconformity with three higher-frequency cycles with varying thicknesses on top of the overall second-order sea-level lowstand (ZSB3; Fig. 8). The geometry of the basin was now more pronounced with establishment of carbonate platforms through thick evaporite deposits rimming the basin (e.g., Füchtbauer 1968; Strohmenger et al. 1996; Kaiser et al. 2003; Slowakiewicz and Mikolajewski 2009). The stacking-patterns of the first two sequences reflect an overall deepening-upward pattern with calcareous varve-laminated mudstone and wackestone in the basin which are followed by organic-rich calcareous mudstones suggesting drowning and retrogradation during the overall sea-level rise. Deepening upward is further manifested in the second cycle where laminated, bituminous mudstones form the TST of higher-frequency cycles that are followed by laminated dolo-mudstones in the slope

and basin. The deepening in the middle of the Z2 cycle has also been observed by Kaiser et al. (2003) on the northern slope of the basin where characteristic smelly carbonate and shale facies (Stinkschiefer, Stinkkalke) developed in euxinic and anoxic environments. The slope shows frequent lime-mud and skeletal calcareous turbidites that occurred during highstand shedding from the platform scouring the organic-rich mudstones. Cross-bedding indicates currents along the slope and basin and possibly wave-action during small-scale sea-level fluctuations. The platform is characterized by shoals rimming the basin and sabkha environments dominating the lagoon. The third sequence (ZSII-3) culminates as a shallowing-upward sequence on the top of the relatively thin (<5 m) Basal Anhydrite followed by thick salt and anhydrite. The halite represents the lowstand systems tract and blanketed most of the basin (Kaiser et al. 2003).

Unconventional reservoir potential

General requirements to classify as shale-oil and/or shale-gas reservoir are TOC contents >2 %, maturity in oil window or above (i.e., Ro > 0.7 and > 1.4 %, respectively), and a minimum thickness of 20 m (depending on many variables including economics), predominant kerogen type II, and a favorable free/adsorbed gas ratio (EMD annual report 2011; Roth 2011). Some of these requirements, but not all, are indeed met by the Z1 and Z2 mudrocks. Hartwig and Schulz (2010) determined that the Z2 basin and slope mudrocks in the Brandenburg area have limited shale-gas potential. This conclusion was based on the low TOC, relatively thin interval of Z2 organic-rich mudrocks, and low hydrocarbon potential. However, additional assessment of Z1 and Z2 basinal and slope deposits present possible unconventional reservoir potential in interfingering packstones and organic-rich mudstones in the Z1 and in the slope deposits of the Z2 microbial organic-rich mudstones (Fig. 9).

Z1 shale-gas/oil potential

Z1 mudrocks were assessed for their shale-oil/gas potential. Z1 mudrocks (i.e., Kupferschiefer) represent oil and gas-generating source rocks in slope and basinal settings (Table 1). Reservoir characterization of these source rocks were performed using Ar-ion milled samples (see Loucks et al. 2012 for technique) under Environmental SEM and SEM, performing XRD, XRF and TOC analyses to assess the character of these mudrocks. The current TOC of limited samples of the Kupferschiefer was determined to range between 2 and 6 % (Fig. 10) and the Hydrogen Index (HI) is in the 100–200 mg HC/g TOC range (Fig. 10). The kerogen type was analyzed to be marine Type II and the maturity ranges from 0.7 to 3.8 % Ro at burial depths from 2,000 m to greater than 4,000 m. The lithologic character is dominated by argillaceous mineralogies such as clay, illite, quartz, calcite, dolomite, albite, pyrite and organic matter (Fig. 10). Porosity and permeability in these heavily compacted mudrocks are low and mainly in micro- and nano-pores of organic matter and interparticle pores (Fig. 9). Thickness of these mudrocks ranges from 30 cm to 1 m across the basin.

Most of the Z1 Kupferschiefer characteristics are similar to shale-gas and shale-oil reservoirs in the US (e.g., Loucks and Ruppel 2007; Hammes et al. 2011; Loucks et al. 2012), however, the overall thickness of the Z1 mudrock is too thin to be a viable candidate for horizontal drilling. However, as an alternative, unconventional reservoir potential is suggested in so-called "hybrid" reservoirs where slightly more porous rocks (i.e., carbonate facies) are sandwiched between organic-rich mudrocks similar to the Bakken Formation, USA (e.g., Fincham and Hill 2011 and references therein). A sandwich-principle may be applied to the Z1 mudrocks because of the evaporitic seal. Interfingering of slightly more porous grain- and packstones with organic-rich mudrocks on the slope might present a hybrid possibility for exploring this organic-rich mudrock (Fig. 11).

Z2 shale-gas/oil potential

The Z2 basinal mudstones were also analyzed using the techniques described above for their shale-gas/oil potential. TOC content of the organic-rich mudstones reach up to 0.88 % in most basinal sections of the ZSII-2 cycle and maturity ranges from 0.7 to 3.8 % Ro at burial depths from 2,000 m to greater than 4,000 m. The lithology is carbonate dominated with calcite and dolomite as prevalent minerals and minor clay, organic matter, feldspars, apatite, biotite, pyrite, and coelestine (Fig. 10). The HI of the basinal mudstones is slightly higher than the Z1 of above 200 mg HC/g TOC (Fig. 10). Kerogen type was analyzed to be of Type II amorphous organic matter with increasing liptinites in less mature samples. The porosity type is primarily in intercrystalline pores (Fig. 9) and ranges 0.8–4 %, and permeability ranges between 0.01 and 1 mD. The overall thickness of the organic-rich carbonates ranges from 8 to 15 m in the basin and up to 30+ meters on the platform. Although the Z2 basinal and slope organic-rich, algal-laminated calcareous and dolomitic mudstones do not match the classic source rock and shale-gas/oil criteria mentioned above, these mudstones are known self-sourced source rocks in the Zechstein Z2 cycle of Poland (e.g., Kotarba et al. 2011; Slowakiewicz and Mikolajewski 2011) and northern Germany (e.g., Gerling et al. 1996b). In addition, oil staining and oil oozing from these deposits are

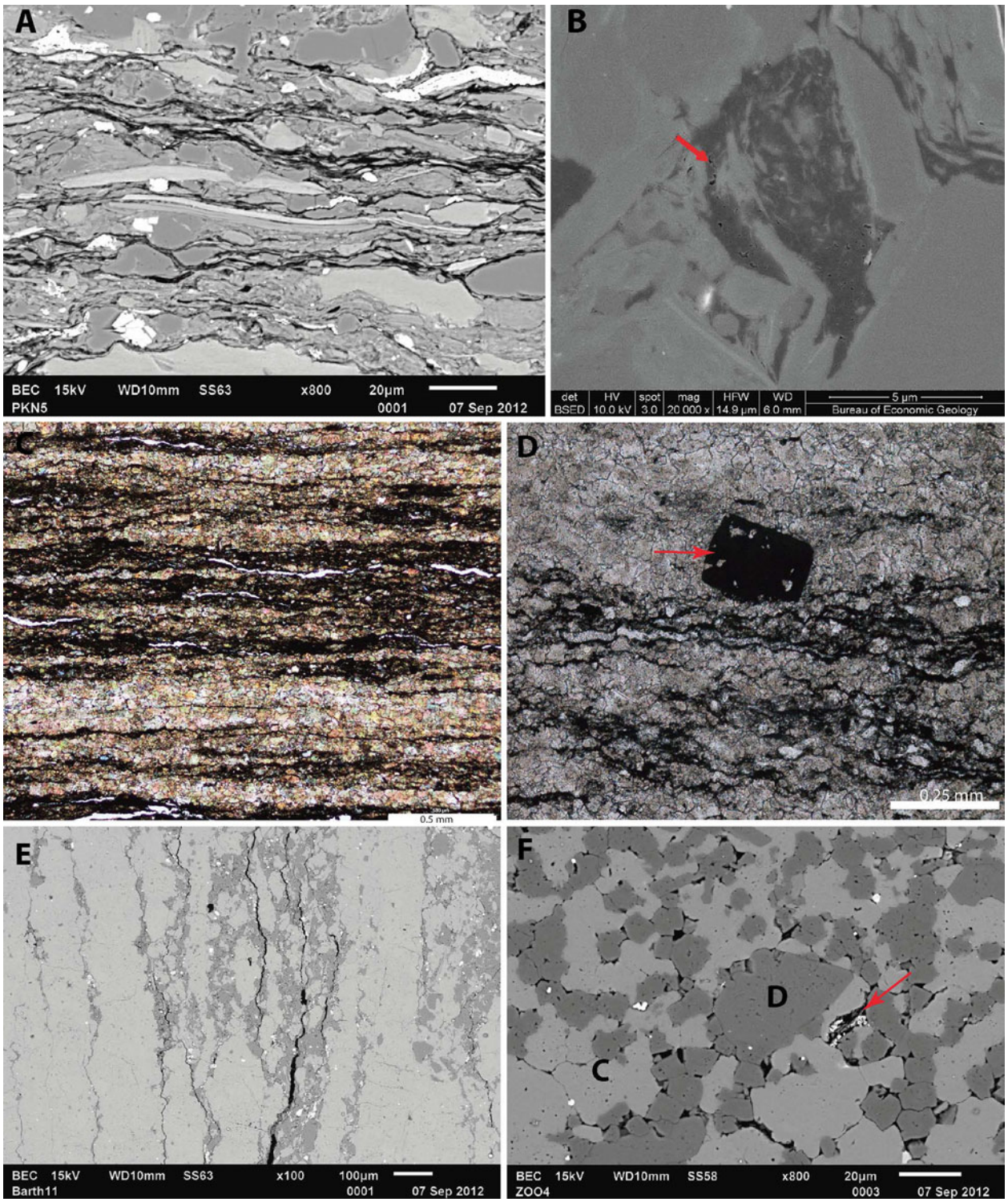

Fig. 9 Reservoir characteristics of Z1 and Z2 organic-rich mudstones: **a** Backscatter SEM image of Z1 Kupferschiefer organic-rich mudstone showing densely compacted layers of calcite, illite, pyrite, albite, clay, and organics. **b** Ar-ion milled backscatter SEM photo of organic material within Kupferschiefer showing nanopores located within the organics (*red arrow*). **c** Laminated organic-rich calcareous mudstone showing layers of calcite (*light colored*) and microbial layers (*black*). White horizontal fractured areas are cracks from sample preparation. **d** Laminated organic-rich mudstone showing layers of organics and bitumen (*black*), dolomitized calcite (*grey*), and a pyrite crystal (*arrow*). **e** Backscatter SEM image of Z2 laminated mudstone showing calcite (*light grey*), dolomite (*dark grey*) and organic layers (*black*). Note that dolomite is concentrated along bedding planes laminated with microbial mats. **f** SEM photograph of dolomitized layer showing interparticle pores (*black*), calcite (C, *light grey*), dolomite (D, *dark grey*), clay filling pores (*red arrow*), and pyrite (*bright specs*). Note porosity between grains but also within crystals

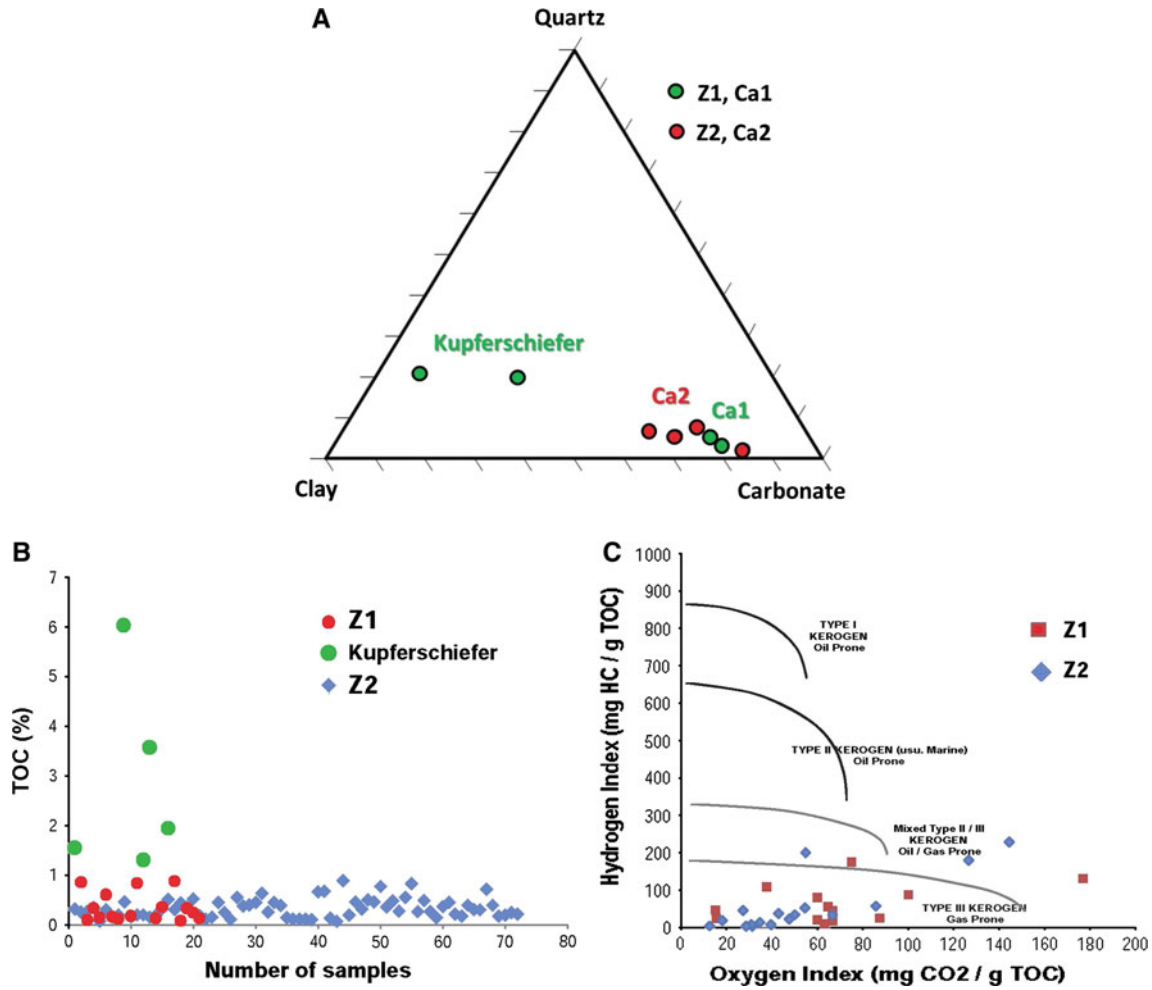

Fig. 10 **a** XRD results from selected Z1 and Z2 mudrock and mudstone samples. The Kupferschiefer T1 source rock has higher clay and quartz but lower carbonate content. The Z2 mudstones and Ca1 carbonates are dominated by carbonate. **b** TOC values for Z1 and Z2 mudstones and Kupferschiefer T1 mudrocks showing the higher TOC in the clay-rich mudrocks. **c** Pseudo-VanKrevelen diagram showing HI versus OI indices of Z1 and Z2 mudstones

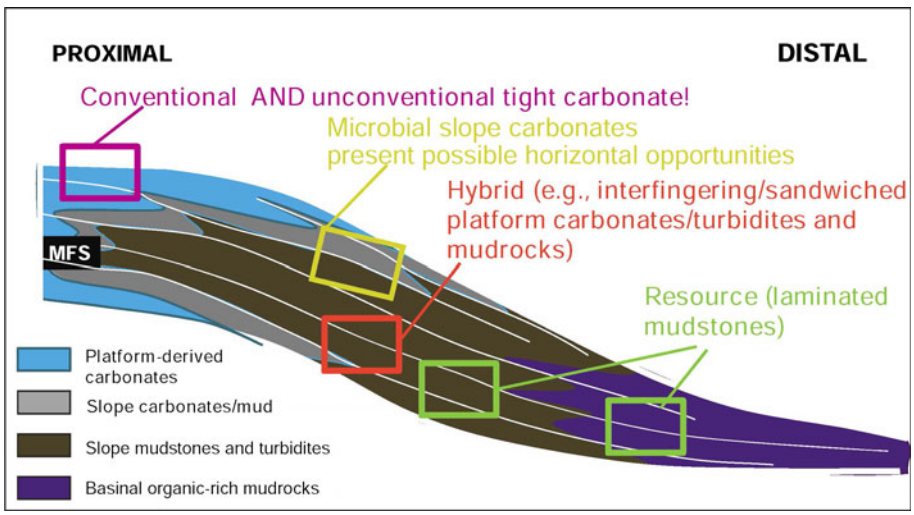

Fig. 11 Conceptual model of Zechstein Z1 and Z2 potential unconventional reservoirs showing interfingering of carbonate and mudrock facies creating potential hybrid reservoirs and microbial slope carbonates for horizontal drilling opportunities

indications of an active hydrocarbon system particularly on the northern slope area of Mecklenburg-Vorpommern (own observations; Schulz and Waldmann 1968). Similar sorts of microbial carbonates are interpreted to source prolific oil and gas reservoirs in the Middle East, the Devonian of Canada, the Paradox Basin of the USA, and others (e.g., Kirkland and Evans 1981; Warren 1986; van Buchem et al. 2005 and references therein). Not only is the preservation potential high, but also the deposition in a mesosaline environment such as the Z2 mudstones favors accumulation of organic matter in restricted basins such as the Epeiric Sea of the Southern Permian Basin.

At first glance, the basinal mudstones exhibit characteristics of shaly source rocks such as fissility, black color, and a strong hydrocarbon smell. However, these mudstones are mainly composed of carbonate with a few accessory minerals rather than the classic carbonate-rich black shale such as the Barnett Shale in Texas (e.g., Loucks and Ruppel 2007) or the Eagle Ford Shale in South Texas (e.g., Driskill et al. 2012) whose lithology are rather clay/silica-rich carbonates. Instead, the basinal Z2 carbonates show evidence of densely laminated organic material on top of calcite and evaporite layers (Fig. 9) similar to modern organic-rich sabkha environments (e.g., Malek-Aslani 1980; Kirkland and Evans 1981). These layers of organic matter are commonly enriched in lipids and therefore present an important contribution to hydrogen-rich kerogen (Gehman 1962; Malek-Aslani 1980). Although today's TOC content is below the requirements for shale-gas criteria, the organic matter that converts to hydrocarbons in carbonate rocks is three to four times higher than in shales (Gehman 1962). This implies that not only the basinal but also the slope microbial carbonates have potential to serve as source rocks (Fig. 11). Therefore, unconventional reservoir development in the slope deposits of the Z2 formation, where tight organic-rich microbial mudstones are within the oil zone, might serve as horizontal drilling targets that might produce economic results.

Conclusions

A sequence stratigraphic and sedimentologic assessment of the Upper Permian Zechstein Group revealed unconventional reservoir potential. Cyclic sedimentation related to relative sea-level fluctuation resulted in deposition of shale-dominated source rocks of the Kupferschiefer that blanketed the Southern Permian Basin from Poland to England. These transgressive shales were subsequently overlain by several cycles of shallow-water carbonates culminating in a thick anhydrite section on the top of the Z1 cycle (e.g., Werra Anhydrite). The platform and lagoon contains thick sections of predominantly dolomite and evaporites resulting from arid to semi-arid climates in the Upper Permian (Roscher and Schneider 2006). Potential unconventional reservoirs as hybrid reservoirs in Z1 interfingering of organic-rich mudrocks and grain-dominated fabrics along the southern and northern slopes. The overlying thick anhydrite section of the Werra series provides a seal for potential tight carbonate reservoirs. The next complete sequence above the Werra Anhydrite continued with evaporitic lithologies of dolomites and limestones across the basin and dolomites on the platform. The transgressive sequence is characterized by organic-rich microbial calcareous mudstones (Stinkschiefer) in the basin and laminated calcareous mudstones on the slope. The platform and lagoonal environments in the Brandenburg area were dominated by microbial-laminated dolomite and anhydrite lithologies. Potential unconventional reservoirs might be explored in laminated organic-rich mudstones within the oil window along the northern and southern slopes of the basin. Although the Zechstein Z1 and Z2 cycles might have limited shale-gas potential because of low thickness and deep burial depth to be economic at this point, unconventional reservoir opportunities that include hybrid and shale-oil potential are possible in the study area.

Acknowledgments This project was supported by the BMBF with the project GeoEn. The senior author would like to thank for the support she received from the GeoEn program at the University of Potsdam, GeoForschungsZentrum Potsdam and the Mudrock Systems Laboratory at the University of Texas at Austin during her research year at the University of Potsdam. The laboratories of Henry Francis, The University of Kentucky, and Necip Gueven, San Antonio, TX, conducted XRF and XRD analyses, respectively. Geomark laboratories of Houston, TX, conducted the Rock–eval analyses. Thanks to the staff at the University of Potsdam, Christine Günther for assistance with the SEM, Christina Fischer for making excellent thin sections and Antje Musiol for furnishing TOC analyses. The senior author would like to thank Dipl. Geol. Max Zitzmann for support during sampling in sub-zero temperatures in different core storage buildings. We are also indebted to Dr. Karsten Obst und Juliane Brandes at LUNG for support and providing access to cores and data as well as to the President of the LBGR, Dr. Klaus Freytag for his support in the study.

References

Anderson RY, Dean WE Jr, Kirkland DW, Snider HJ (1972) Permian castile varved evaporite sequence, West Texas and New Mexico. Geol Soc Am Bull 83–1:59–86

Bechtel A, Püttmann W (1997) Paleoceanography of the early Zechstein Sea during Kupferschiefer deposition in the Lower Rhine Basin (Germany): a reappraisal from stable isotope and organic geochemical investigations. Palaeogeogr Palaeoclimatol Palaeoecol 136:331–358

Bechtel A, Gratzer A, Püttmann W, Oszczepalski S (2000) Geochemical and isotopic composition of organic matter in the Kupferschiefer of the Polish Zechstein basin: relation to maturity and base metal mineralization. Int J Earth Sci 89:72–89

Becker F (2002) Zechsteinkalk und Unterer Werra-Anhydrit (Zechstein 1) in Hessen: Fazies, Sequenzstratigraphie und Diagenese. Geologische Abhandlungen Hessen 109:1–231

Becker F, Bechstädt T (2006) Sequence stratigraphy of a carbonate-evaporite succession (Zechstein 1, Hessian Basin, Germany). Sedimentology 53:1083–1120. doi:10.1111/j.1365-3091.2006.00803.x

Dyjaczynski K, Gorski M, Mamczur S, Peryt TM (2001) Reefs in the basinal facies of the Zechstein limestone (Upper Permian) of western poland a new gas play. J Pet Geol 24–3:265–285

Driskill B, Garbowicz A, Govert AM, Suurmeye N (2012) Reservoir description of the subsurface Eagle FordFormation, Maverick Basin area, South Texas, USA. In: 74th EAGE conference & exhibition incorporating SPEEUROPEC 2012 Conference and Technical Exhibition - European Association of Geoscientists and Engineers, Society of Petroleum Enginners, 4–7 June 2012

Fincham B and Hill D (2011) Bakken–the biggest oil resource in the United States? DOE NETL, E&P Focus. Winter 1:3–17

Füchtbauer H (1968) Carbonate sedimentation and subsidence in the Zechstein Basin (northern Germany) Germany. In: Füchtbauer H (ed) Recent developments in carbonate sedimentology in central Europe. Springer, New York, pp 196–204

Gaupp R, Gast R, Forster C (2000) Late Permian Playa Lake Deposits of the Southern Permian Basin (Central Europe). In: Gierlowski-Kordesch EH, Kelts KR (eds) Lake basins through space and time: AAPG Studies in Geology, vol 46, pp 75–86

Gebhardt U, Schneider J, Hoffmann N (1991) Modelle zur Stratigraphie und Beckenentwicklung im Rotliegend der Norddeutschen Senke. Geologisches Jahrbuch Reihe A 127:405–427

Gehman HM Jr (1962) Organic matter in limestones. Geochemica et Cosmochimica Acta 2:885–894

Geluk MC (2000) Late Permian (Zechstein) carbonate-facies maps, the Netherlands. Geologie en Mijnbouw Netherlands J Geosci 79–1:17–27

Geluk MC (2005) Stratigraphy and tectonics of Permo-Triassic basins in the Netherlands and surrounding areas. Dissertation, University Utrecht

Geluk MC (2007) Permian. In: Wong ThE, Batjes DAJ, De Jager J (eds) Geology of the Netherlands. Royal Dutch Academy of Arts and Science, Amsterdam, pp 59–79

Gerlach R, Knitzschke G (1978) Sedimentationszyklen an der Zechsteinbasis (Z1) im SE Harzvorland und ihre Beziehung zu einigen bergtechnischen Problemen. Zeitschrift der angewandten Geologie 24:214–221

Gerling P, Piske J, Rasch H-J, Wehner H (1996a) Paläogeographie, Organofazies und Genese von Kohlenwasserstoffen im Staßfurt-Karbonat Ostdeutschlands-Teil 1 Sedimentationsverlauf und Muttergesteinsausbildung. Erdöl Erdgas Kohle 112–1:13–18

Gerling P, Piske J, Rasch H-J, Wehner H (1996b) Paläogeographie, Organofazies und Genese von Kohlenwasserstoffen im Staßfurt-Karbonat Ostdeutschlands-Teil 2 Genese Erdölen und Erdölbegleitgasen. Erdöl Erdgas Kohle 112–4:152–156

Hammes U, Hamlin HS, Ewing TE (2011) Geologic analysis of the upper Jurassic Haynesville shale in East Texas and West Louisiana. AAPG Bull 95–10:1643–1666

Haq BU, Hardenbol J, Vail PR (1988) Mesozoic and Cenozoic chronostratigraphy and cycles of sea-level change. In: Wilgus CK, Hastings BS, Kendall CGSTC, Posamentier HW, Ross CA, Van Wagoner JC (eds) Sea level changes. An integrated approach. SEPM Special Publication, Tulsa, vol. 42, pp 71–108

Hartwig A, Schulz H-M (2010) Applying classical shale gas evaluation concepts to Germany: Part I: The basin and slope deposits of the Stassfurt Carbonate (Ca2, Zechstein, Upper Permian) in Brandenburg. Chemie der Erde–Geochem 70(3):77–91

Janson X, Kerans C, Playton T, Clayton J, Winefield P, Burgess P (2012) Stratigraphic models and exploration plays of slope and basin-floor carbonates. Search Discov Art #50637

Käding K-C (2000) Die Aller- Ohre, Friesland und Fulda-Folge (vormals Bröckelschiefer-Folge). Kali u. Steinsalz 13:760–770

Kaiser R, Nöth S, Ricken W (2003) Sequence stratigraphy with emphasis on platform-related parasequences of the Zechstein 2 carbonate (Ca2)—the northern platform margin of the Southern Permian Basin (NE Germany). Int J Earth Sci 2000(92):54–67

Karnin WD, Idiz E, Merkel D, Ruprecht E (1996) The Zechstein Stassfurt carbonate hydrocarbon system of the Thuringian Basin, Germany. Petrol Geosci 2:53–58

Kennard JM, James NP (1986) Thrombolites and stromatolites: two distinct types of microbial structures. Palaios 1:492–503

Kirkland DW, Evans R (1981) Source-rock potential of evaporitic environment. AAPG Bull 65–2:181–190

Kopp J, Simon A, Göthel M (2006) Die Kupferlagerstätte Sprembergh-Graustein in Südbrandenburg. Brandenburg. Geowissenschaftliche Beiträge 13–1(2):117–132

Kotarba MJ, Wagner R (2007) Generation potential of the Zechstein Main Dolomite (Ca2) Carbonates in the Gorzo′w Wielkopolski–Miedzycho′ d–Lubiato ′w area, geological and geochemical approach to microbial-algal source rock. Polish Geol Rev 2(1):1025–1036

Kotarba MJ, Peryt TM, Koltun YV (2011) Microbial gas system and prospective of hydrocarbon exploration in Miocene strata of the Polish and Ukrainian Carpathian Foredeep. Ann Soc Geol Pol 81:523–548

Legler B, Gebhardt U, Schneider JW (2005) Late Permian non-marine–marine transitional profiles in the central Southern Permian Basin, northern Germany. Int J Earth Sci 94:851–862

Leyrer K, Strohmenger C, Rockenbauch K, Bechstaedt T (1999) High-resolution forward stratigraphic modeling of Ca2-carbonate platform and off-platform highs (Upper Permian Northern Germany). In: Harff J, Lemke W, Stattegger K (eds) Computerized modeling of sedimentary systems, Springer, Hiedelberg, pp 307–339

Lokhorst A (1997) The Northwest European Gas Atlas. Netherlands Institute of Applied Geoscience, Haarlem

Loucks RG, Ruppel SC (2007) Mississippian Barnett Shale: lithofacies and depositional setting of a deep-water shale-gas succession in the Fort Worth Basin, Texas. AAPG Bull 91–4:579–601

Loucks RG, Reed RM, Ruppel SC, Hammes U (2012) Spectrum of pore types and networks in mudrocks and a descriptive classification for matrix-related mudrock pores. AAPG Bull 96–6:1071–1098

Malek-Aslani M (1980) Environmental and diagenetic controls of carbonate source rocks. AAPG Bull 64:744–745

Menning M, Gast R, Hagdorn H, Käding K-C, Szurlies M, Nitsch E (2005) Die Zeitskala für die höhere Dyas und die Germanische Trias der Stratigraphischen Tabelle von Deutschland 2002. Newsl Stratigr 41:173–210

Müller EP, Dubslaff H, Eiserbeck W, Sallum R (1993) Zur Entwicklung der Erdöl-und Erdgasexploration zwischen Ostsee und Thüiringer Wald. In: Müller EP and Porth H (eds) Zur Geologie und Kohlenwasserstoffführung des Perm im Ostteil der Norddeutschen Senke: Geologisches Jahrbuch A 131:5–30

Mutti M, Weissert HJ (1995) Climate cyclicity and monsoons in the Triassic Pangea: the sedimentological and isotopic record from Ladinian–Carnian carbonate platforms (Southern Alps, Italy). J Sediment Res B 65–3:357–367

Paul J (1986a) Environmental analyses of basin and schwellen facies in the lower Zechstein of Germany. In: Harwood GM, Smith DB (eds) The English Zechstein and related topics. Geological Society, London. Special Publications, vol. 22, pp 143–147. doi:10.1144/GSL.SP.1986.022.01.02

Paul J (1986b) Stratigraphy of the Lower Werra Cycle (Z1) in West Germany (preliminary results). In: Harwood GM, Smith DB (eds) The English Zechstein and related topics. Geological Society, London. Special Publications, vol. 22, pp 149–156. doi:10.1144/GSL.SP.1986.022.01.02

Paul J (1991) Zechstein carbonates–Marine episodes of a hypersaline sea. Zentralblatt für Geologie und Paläontologie Teil 1–4:1029–1045

Paul J (2006) Der Kupferschiefer Lithologie. Stratigraphie, Fazies und Metallogenese eines Schwarzschieferes, ZDGG 157–1:57–76

Peryt TM (1986) Chronostratigraphical and lithostratigraphical correlations of the Zechstein Limestone of Central Europe. In: Harwood GM, Smith DB (eds) The English Zechstein and related topics. Geological Society, London. Special Publications, vol. 22, pp 201–207. doi:10.1144/GSL.SP.1986.022.01.02

Peryt TM, Orti F, Rosell L (1993) Sulfate platform basin transition of the lower Werra Anhydrite (Zechstein, Upper Permian), western Poland: facies and petrography. J Sediment Petrol 63:646–658

Peryt TM, Geluk MC, Mathiesen A, Paul J, Smith K (2010) Zechstein. In: Doornenbal JC, Stevenson AG (eds) Petroleum Geological Atlas of the Southern Permian Basin Area. EAGE Publications b.v, Houten, pp 123–147

Peryt TM, Raczinski P, Peryt D, Chlodek K (2012) Upper Permian reef complex in the basinal facies of the Zechstein Limestone (Ca1), western Poland. Geol J 47–5:537–552. doi:10.1002/gj2440

Playton TE, Kerans C (2002) Slope and Toe-of-slope deposits shed from a Late Wolfcampian tectonically active carbonate ramp margin. Gulf Coast Assoc Geol Soc Trans 52:811–820

Plein E (1994) Germany. In: Kulke H (ed) Regional petroleum geology of the world, Part I: Europe and Asia. Gebrüder Borntraeger Verlagsbuchhandlung, Stuttgart, pp 139–192

Rentzsch J (1965) Die feinstratigraphisch-lithologische Flözlagenparallelisierung im Kupferschiefer am Südrand des norddeutschen Becken. Zeitschrift angewandte Geologie 11:11–14

Richter-Bernburg G (1955) Stratigraphische Gliederung des deutschen Zechsteins. Zentralblatt der Deutschen Geologischen Gesellschaft 105:843–854

Richter-Bernburg G (1982) Stratogenese des Zechsteinkalkes am Westharz. Zentralblatt der Deutschen Geologischen Gesellschaft 133: 381-40 Richter-Bernburg, G., 1982. Stratogenese des Zechsteinkalkes am Westharz. Z Dtsch Geol Ges 133:381–384

Richter-Bernburg G (1985) Zechstein-Anhydrite–Fazies und Genese. Geologisches Jahrbuch, Reihe A-85

Roscher M, Schneider JW (2006) Permo-Carboniferous climate: Early Pennsylvanian to Late Permian climate development of central Europe in a regional and global context. Geol Soc Lond Special Publ 265:95–136. doi:10.1144/GSL.SP.2006.265.01.05

Roth M (2011) North American shale gas reservoirs: similar, yet so different. AAPG (American Association of Petroleum Geologists) Convention, Calgary. Search Discov Art #80136

Scheck-Wenderoth M, Lamarche J (2005) Crustal memory and basin evolution in the Central European Basin System: new insights from a 3D structural model. Tectonophysics 397:143–165

Schulz G, Waldmann R (1968) Ausführliches Schichtenverzeichnis der Bohrung Prerow 1/65. VEB Erdöl und Erdgas Grimmen

Slowakiewicz M, Mikolajewski Z (2009) Sequence stratigraphy of the Upper Permian Zechstein Main Dolomite carbonates in Western Poland: a new approach. J Pet Geol 32–3:215–233

Slowakiewicz M, Mikolajewski Z (2011) Upper Permian Main Dolomite microbial carbonates as potential source rocks for hydrocarbons (W Poland). Mar Pet Geol 28:1572–1591

Smith DB, Harwood GM, Pattison J, Pettigrew TH (1986) A revised nomenclature for Upper Permian strata in eastern England. In: Harwood GM, Smith DB (eds) The English Zechstein and related topics. Geological Society, London. Special Publications, vol. 22, pp 9–12. doi:10.1144/GSL.SP.1986.022.01.02

Steinhoff I, Strohmenger C (1996) Zechstein 2 carbonate platform subfacies and grain-type distribution (Upper Permian, Northwest Germany). Facies 35:105–132

Strohmenger C, Voigt E, Zimdars J (1993) Einfluß von Eustasie und Paläorelief auf die sedimentologische und diagenetische Entwicklung der Zechstein 2 Karbonate (Ober-Perm, Nordost-Deutschland). Erdöl Erdgas Kohle 109–11:445–450

Strohmenger C, Voigt E, Zimdars J (1996) Sequence stratigraphy and cyclic development of Basal Zechstein carbonate-evaporate deposits with emphasis on Zechstein 2 off-platform carbonates (Upper Permian, Northeast Germany). Sed Geol 102:33–54

Szurlies M (2013) Late Permian (Zechstein) magnetostratigraphy in Western and Central Europe. In: Gasiewicz A, Slowakiewicz M (eds) Palaeozoic climate cycles: their evolutionary and sedimentological impact. Geological Society, London. Special Publications, vol. 376. doi:10.1144/SP376.7

Tucker ME (1991) Sequence stratigraphy of carbonate-evaporate basins: models and application to the Upper Permian (Zechstein) of northeast England and adjoining North Sea. J Geol Soc Lond 148:1019–1036

Vail PR, Mitchum RM, Thompson III S (1977) Seismic stratigraphy and global changes of sea level: Part 3. Relative changes of sea level from coastal onlap. In: Payton CW (ed) Seismic stratigraphy applications to hydrocarbon exploration. AAPG Memoir, vol. 26, pp 63–97

van Buchem FSP, Huc AY, Pradier B, Stefani MM (2005) The deposition of organic-carbon-rich sediments: models, mechanisms, and consequences. In: Harris NB (ed) Special publication. Society for Sedimentary Geology, vol. 82, pp 191–223

van Wees J-D, Stephenson RA, Ziegler PA, Bayer U, McCann T, Dadlez R, Gaupp R, Narkiewicz M, Bitzer F, Scheck M (2000) On the origin of the Southern Permian Basin, Central Europe. Mar Pet Geol 17:43–59

Wagner R (ed) (2008) Stratigraphic Chart of Poland. Warsaw

Wagner R, Peryt TM (1997) Possibility of sequence stratigraphic subdivision of the Zechstein in the Polish Basin. Geol Quart 41:457–474

Warren JK (1986) Shallow-water evaporitic environments and their source rock potential. J Sediment Res 56:442–454

Ziegler PA (1990) Geological Atlas of Western and Central Europe. Shell International Petroleum Mij BV, 2nd edn. Geological Society Publishing House, London, pp 1–239